Title: Monte Carlo Assessment of Natural Unit Base Power Law Mass Force Hierarchy of Hydrogen on the Minkowski $\mathbb{Z}^2$ Lattice

D. W. Chakeres[1], S. A. Mardan[2], V. Andrianarijaona[3]

[1a)] The Ohio State University, Columbus, Ohio, 43210 USA
[1b)] Electronic mail: donchakeres@gmail.com, https://orcid.org/0000-0002-9495-394X

[2a)]University of Management and Technology, Lahore, Pakistan.
[2b)]Center for Theoretical Physics, Khazar University, 41 Mehseti Str., Baku, AZ1096, Azerbaijan

[2c)]Electronic mail: syedalimardanazmi@yahoo.com,

[3a)]School of Engineering and Physics
[3b)]Southern Adventist University, Collegedale, TN 37315-0370 USA
[3c)]Electronic mail: avola@southern.edu

Abstract:

The origin of the mass–force hierarchy remains one of the major open questions in fundamental physics, since the Standard Model (SM) does not explain the observed pattern of particle masses or the significant differences in interaction strengths. In this work, we examine whether fundamental constants, written as natural-unit (NU) frequency scalars, display an underlying constrained integer-scaling power structure. To explore this idea, we use Hermann Minkowski to approximate ratios of logs of constants by simple rational exponents i/j on a two-dimensional integer lattice. The leading first approximations define scaling relations characterized by parsimonious integer ratios, Diophantine residuals, and a conformal factor frequency ν_{cf}, which measures departures from exact power laws. We apply this framework to hydrogen, using all as the references to the others, but focus on the Rydberg frequency to compare electromagnetic and gravitational quantities as an example. We find that all the exponents are near perfect partial harmonic fractions in a highly structured form when the gravitational binding energy of the electron in hydrogen or the proton are the references. Any ratio of two constants are naturally encoded by the same integers i , j, ν_{cf}, and either constant scalar utilizing a standard algebraic power structure. Monte Carlo tests demonstrate that this ensembles' patterns are unlikely to arise in randomized datasets. These results indicate that part of the hierarchy among fundamental constants may be captured by simple rational scaling relations based on resonant nodes, without altering established SM values.

Key words: Mass–force hierarchy; Number theory; Integer power laws; Minkowski geometry of numbers; Rydberg constant; Hydrogen atom; Electromagnetic–gravitational interaction; Diophantine approximation; Natural units; Computational analysis

1. Introduction

The development of physics has followed the route of analyzing phenomenological data and attempting to accurately define that pattern by a mathematical formulation. Frequently the math formulation was well known and its correspondence to the physical system was clear. On the

other hand, the math may be well known, but there was no known associated physical system. This was true for Riemann's curved space math until it became essential to define relativity [1]. Other times the math is created directly answering issues related to physics such as Minkowski's spacetime and relativity [2]. We combine a number of known math-physical structures to approach the question of the mass-force scale hierarchy. They are all part of the Standard Model, but their combined utilization has not been described. These patterns include the following examples that are analogous to what are found within our methods. Arrhenius described a linear logarithmic plots between temperature and chemical reaction rates [3]. Rydberg described the hydrogen spectrum based on an infinite consecutive integer series of the squares of the harmonic fraction series [4]. Harmonic, (1/n) and partial harmonic fractions (1±1/n) are commonly encounter in physical and quantum resonant systems [5]. Mean motion resonance in planetary systems (like the moons of Jupiter) operates on a series of partial fractions (2:1, 3:2, 4:3) [6]. Meradian described cosmic spin properties based on the mass of the proton and partial harmonic fraction exponents 1+1/2 (3/2), 1+1/3 (4/3) that correlate with the logarithmic scale of galaxies, planets and asteroids linking quantum and cosmic properties together over large scale ranges [7]. Hofstadter's butterfly is a fractal energy spectrum that describes the quantum behavior of 2D electrons subjected to a strong, perpendicular magnetic field within a lattice structure [8]. It is intimately tied to Minkowski's number theory, continued fractions, Farey sequences and Diophantine residuals. The Fowler-Nordheim (FN) Tunneling relationship is related to a partial harmonic fraction power (3/2) of an energy height [9]. Density of States (DOS) quantum states within a lattice are related to energies raised to the power series of ½, 0, and -1/2 [10].

In the SM, fermion masses, mixing parameters and interaction couplings are not calculated, but are measured experimentally [11]. Despite the spectacular success of the theory in a broad spectrum of energies, the theory fails to provide the large-scale separations between observed mass scales, as well as the hierarchy of interaction strengths over many orders of magnitude [12,13]. This deficiency is directly connected with the hierarchy and naturalness issues, which continue to be the main concerns in high-energy physics [14,20,21.25,26].

The relative strengths of interactions can be well described by dimensionless quantities like the fine-structure constant, but the overall scale structure of the SM does not exhibit any obvious unifying integer scaling structure [16]. The theory is flexible enough to allow these parameters, although it does not give any explanation as to why they have the observed values or whether there are more profound relationships between them. This encourages the fact that the hierarchy of scaling of the fundamental constants could be due to an underlying organizing principle of mathematically constrained dimensionless relations or hidden scaling behavior [17,27,58].

The empirical relation between the charged leptons that was proposed by Yoshio Koide was one of the first indications that fermion masses could have hidden structure [12]. The relationship provides a value of 2/3, which is very close to the experimental value, in a nonlinear combination of the electron, muon, and tau masses. This quantitative triumph has inspired a host of theoretical explanations and model construction [23,24]. Nevertheless, even though it is accurate, the Koide relation has not evolved into a general predictive theory of particle masses or has given a systematic explanation of hierarchy patterns in various sectors. Consequently, the larger hierarchy

issue continues to be tackled by further symmetries, mechanisms, or new degrees of freedom on top of the SM [12,13,25].

In this paper we consider another possibility: that the scaling hierarchy between fundamental constants that we observe is due to inherent mathematical structure well described within Number Theory, and not to new dynamical components. In particular, we consider the existence of simple rational scaling relations of constants in the form of NU frequency scalars, and the constraints of parsimony, integer fraction structure, prime factors, resonant power nodes, and geometry. Our model uses Hermann Minkowski Geometry of Numbers, GON, and Diophantine approximation, where the logarithmic ratios of constants are expressed in terms of irreducible rational powers i/j on an integer lattice [29-34]. Irrational exponents cannot be precisely plotted on a integer lattice thus deviations are measured by a residual term and a conformal factor frequency v_{cf}, which is a mapping between the discrete lattice representation and the continuous physical space [46-50].

We use Monte Carlo tests to test whether the observed hydrogen constant scalar Natural Unit, NU, values are significantly different than randomized datasets [51-55]. Assuming that the constants were numerically or mathematically uncorrelated, there would be no low-order rational or prime factor structure to expect. On the other hand, statistically significant deviations of the random expectations would indicate a constrained scaling pattern. In the current analysis, the electromagnetic and gravitational quantities are compared in a common and analytically transparent system, namely hydrogen as an example. We do not intend to assert clear causality, but to explore the possibility that simple arithmetic structure can encode some of the observed mass force hierarchy defining the dimensionless ratios of the constants' scalar values analogous to the original Rydberg series observation.

Besides his contribution to the geometric formulation of special relativity, Hermann Minkowski also contributed to Number Theory, with the Geometry of Numbers, GON, which investigates the connection between continuous quantities and discrete integer lattices [29]. One of the main issues in this context is the representation of an irrational number α by rational fractions i/j, i and j being integers. This is directly related to classical Diophantine approximation results, such as the approximation theorem of Dirichlet [30,33], which guarantees the existence of infinitely many rational approximants of

$$| \alpha - \frac{i}{j} | < \frac{1}{j^2}. \qquad (1)$$

There is a precise representation of some pair (i, j) of rational α. In the case of irrational α, there can be no exact equality, and every rational approximation has a finite residual. In the current work, this discrepancy is represented by the Diophantine residual D_r, which is the difference between the actual logarithmic exponent and one of the infinite possible the rational approximations. By succeeding in increasing the size of integers, one gets an infinite series of better approximants, with smaller residuals, but not necessarily in a monotonic order [30-34].

These integer approximants can be geometrically represented on a two-dimensional integer lattice with coordinates (j, i). The line $y = \alpha x$ only intersects the lattice approximately, convergences, and the local minimum of the residual is a rational fraction i/j, which is locally minimized by the

lattice points. This lattice interpretation gives the mathematical foundation of the discrete scaling relations that are studied in the current analysis.

Figure 1. Possible partial harmonic fractions and specific i/j values for hydrogen from the perspective of v_{R_∞}. Any hydrogen constant could be the point of perspective, and the points and slopes would be different.

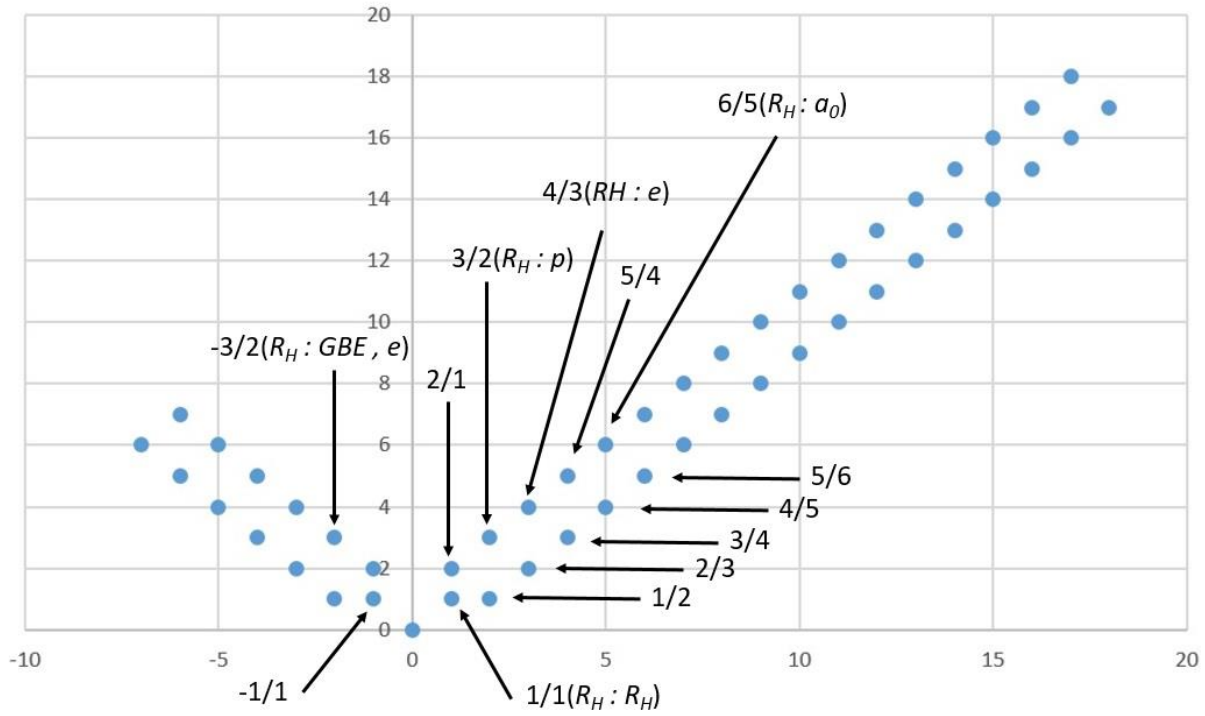

Figure 1 shows the Minkowski GON lattice $\mathbb{Z}^2$ for first-order rational power-law approximants. For target values lying in the approximate interval $v_{R_\infty}^{1/2} \le v \le v_{R_\infty}^{3/2}$, the only admissible first approximants are partial harmonic fractions, PHF, of the form $1 \pm 1/j$, together with the identity points ± 1. Each blue point represents an allowed irreducible pair (i, j), whose only possible corresponding lattice slopes are i/j. For the hydrogen constants referenced to v_{R_∞}, the identified low-order lattice locations are $1/1$ for $(R_\infty : R_\infty)$, $-3/2$ for $(R_\infty : \mathrm{GBE}_e)$, $3/2$ for $(R_\infty : p)$, $4/3$ for $(R_\infty : e)$, and $6/5$ for $(R_\infty : a_0)$. These points illustrate that the selected constants map into a compact subset of simple rational exponents near the unit-slope branch. Other PHF points not associated with constants are labeled as well demonstrating the progression of the infinite rational PHF series.

Figure 2. Geometry-of-Numbers (GON) representation of the hydrogen scaling exponents and associated slopes of the log(target)/log(reference) on the Minkowski lattice $\mathbb{Z}^2$ for the target of gravitational binding energy of the electron in hydrogen, GBE_e, and the reference Rydberg constnt, R_∞.

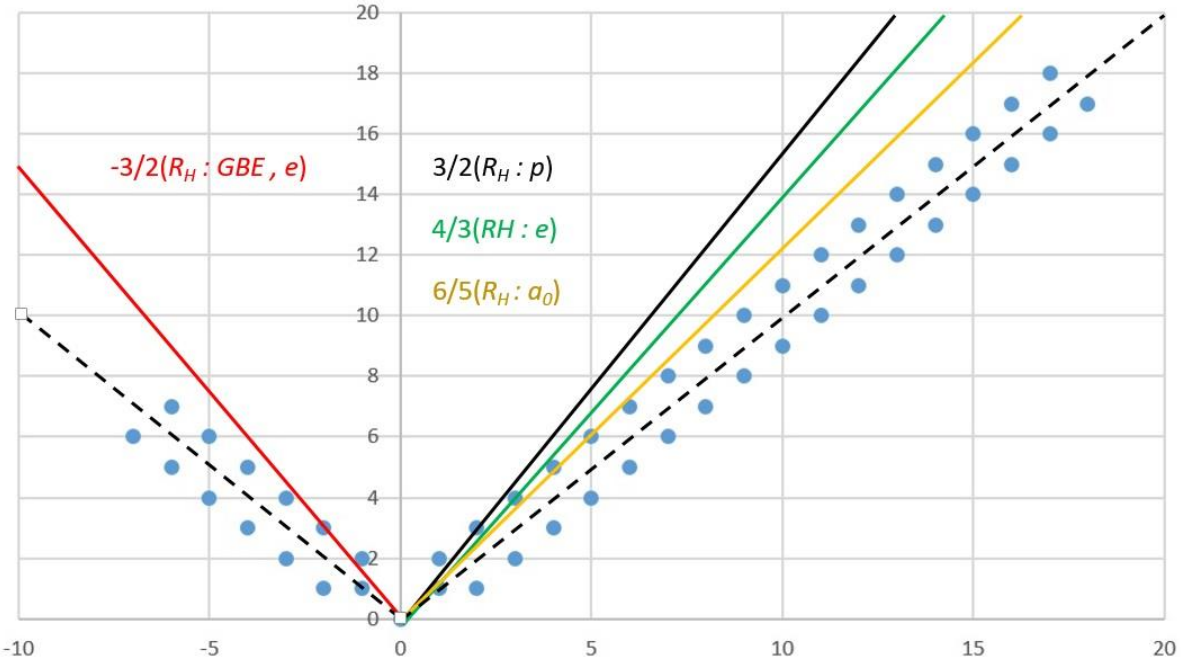

Figure 2 displays the GON integer lattice $\mathbb{Z}^2$ together with the line slopes corresponding to the selected hydrogen constants referenced to v_{R_∞}. For values in the approximate interval $v_{R_\infty}^{1/2} \leq v \leq v_{R_\infty}^{3/2}$, the only admissible first-order lattice points follow the partial harmonic fraction, PHF, sequence, together with the identity points ± 1. Blue markers denote possible allowed irreducible pairs (i, j), while the slope associated with each point is given by the rational exponent i/j. The highlighted lines correspond to the principal hydrogen relations: 1 for $(R_\infty : R_\infty)$ (dashed black) or -1, $-3/2$ for $(R_\infty : \mathrm{GBE}_e)$ (red), $3/2$ for $(R_\infty : p)$ (solid black), $4/3$ for $(R_\infty : e)$ (green), and $6/5$ for $(R_\infty : a_0)$ (gold). Each relation is represented by a distinct slope, illustrating how the selected constants occupy separate unique low-order branches of the lattice. For this scalar hydrogen range of numerical values the only possible valid points are between the slopes of 1 and 3/2.

Since i/j is taken to be an irreducible rational ratio, its prime-factor structure naturally characterizes the associated scaling relation. Emphasizing the smallest admissible integers is consistent with the spirit of Hermann Minkowski and with classical minimality principles frequently used in mathematics and physics [29,30,32,34]. The first point, most parsimonious, of an infinite series related to an irrational slope is defined as the fundamental within the GON. In the present framework, the mass–force hierarchy is therefore examined through the fundamental parsimonious pair (i, j), together with the requirement that the corresponding relation be exact or nearly exact.

For near-perfect power laws, the Diophantine residual D_r must be small, while the conformal factor frequency v_{cf} should remain close to unity in the adopted NU normalization. A perfect power law has a v_{cf} of 1 Hz, and a D_r of zero. In this sense, v_{cf} provides a quantitative dimensioned measure of how closely two constants approach an exact rational scaling relation. It is not

introduced as a fitting parameter, but is strictly mathematically self-emergent. It is out of control of the observer. It is a transformation factor mapping between the discrete integer dimensionless lattice representation and the continuous frequency domain. Similar connections between discrete structure and continuous scaling appear broadly in renormalization and self-similar systems [27,41,42].

The simultaneous necessity of low-order integers, small D_r residuals, and $v_{\mathrm{cf}} \approx 1$ puts a nontrivial constraint on the scalar data of a group of numbers that would not be anticipated of arbitrary numerical data. The lower the integers the larger the v_{cf} range must be encountered in a random system. Larger integers would be uncommon with a probability of approximately $1/j^2$. This is in line with classical findings in Diophantine approximation, where the distribution and quality of rational approximants is systematically dependent on the denominator j [30,31,33]. We thus evaluate statistical significance with respect to randomized controls by conventional Monte Carlo techniques [51-55]. If the fundamental constants scalars are random, not organized within a GON structure, then the integers, D_r, and v_{cf} structure that those mathematically represents is an exact isomorphic form of the scalars would be expected to be random in nature as well.

One of the main reasons to study the hydrogen system is that the NU frequency of the electron gravitational binding energy is numerically similar to the reciprocal of the proton frequency. This mathematical scalar relationship must be within a near perfect integer power law system. This encourages the generalization of the analysis to other constants of hydrogen, such as the electron mass, Bohr radius, and Rydberg scale, in a shared lattice structure. Hydrogen is especially clean as its structure is theoretically well understood and its constants are known with high precision within the Bohr model algebraic geometric relationships [56,57].

Such comparisons are independent of arbitrary unit conventions and are based solely on relative scale structure when expressed in natural units, NU, [16,18,58-60]. In this regard, the current research is concerned with the first and most parsimonious rational approximant in the Minkowski sequence of each pair of constants cross analyzing all of them as the reference. When low-order relations are observed to be consistent across multiple instances, then they can be a sign of an underlying organizational pattern in the hierarchy observed, and not a mere coincidence of numbers [19,27,35,36]. We focus on the gravitational binding energy of the electron and the Rydberg constant, but all of the constants are evaluated from their reference perspective to all of the rest.

Figure 3. First-order Minkowski parsimony lattice pattern obtained from Monte Carlo sampling.

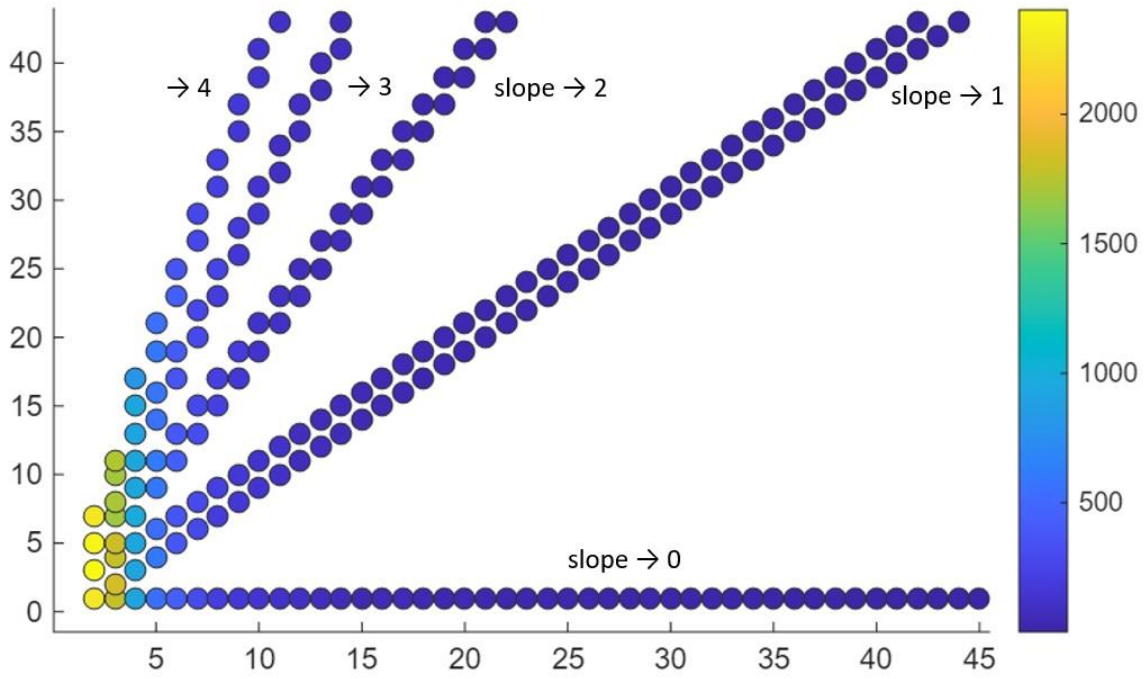

Figure 3 illustrates the distribution of leading fundamental most parsimonious rational approximants on the integer lattice $\mathbb{Z}^2$, generated from a Monte Carlo scan of randomly sampled target frequencies relative to a fixed reference value. For each trial, the logarithmic slope $\log(v_{\text{random target}})/\log(v_{\text{ref}})$was computed for a range of $v_{ref}^{1/45}$ to $v_{ref}^{4.5}$, and the first locally optimal rational approximant i/jminimizing the Diophantine residual $D_r$was identified. Colors indicate the relative frequency of occurrence, with warmer colors denoting more common outcomes and darker colors fewer common ones.

The resulting pattern is highly structured, Fig (1). For target scales smaller than $v_{\text{ref}}^{1/2}$, the dominant first approximants follow the sequence $1/j$, approaching zero slope. In the approximate interval $v_{\text{ref}}^{1/2} \leq v \leq v_{\text{ref}}^{3/2}$, the allowed first approximants form the partial harmonic fraction branch centered on unit slope. Higher target ranges generate analogous branches around successive integer slopes approaching integer values of (0,1,2,3, ...).

This geometric progression converts a continuous slope system into a combined integer fraction and irrational D_r system, just as the Minkowski method does. There are an infinite number of possible slopes, but limited to narrow integer bands. The first Minkowski approximant maps a continuous range of scale ratios onto an ordered sequence of low-integer rational classes, with the residual $D_r$encoding the remaining continuous deviation from exact rational scaling.

The admissible i/j pattern depends on the logarithmic ratio of a selected reference and target values of a group of numbers, and its qualitative structure is not dependent on the base of the logarithm. The range of the slopes define the possible i/j possibilities. The rescaling of the base only rescales the representation, but does not change the underlying ordering of rational approximants [30-34]. In the current work, NU frequency scalars are used in such a way that

arbitrary unit conventions are eliminated and only scale relations that are dimensionless are left [16,18,58]. Within the constraint of the first parsimonious approximant, the target values that are positive are all linked to a single leading rational slope i/j with a residual D_r. This results in a discrete mapping of a continuous scale of numerical scales to a discrete lattice of low-integer rational classes as shown in Fig. 3. The dominant rational approximation is determined by the lattice coordinates (i, j) and D_r measures the rest of the continuous deviation of the exact scaling.

The branches of the first order that are admissible are arranged around successive integer slopes $(\dots, -2, -1, 0, 1, 2, \dots)$, but most approximants are close to, but not on these lines unless they are perfect power laws with v_{cf} equals 1 Hz. This hierarchical bifurcation is a natural result of rational approximation of integer lattices and is a geometry of continued fraction convergent [30-33].

When the target values are such that $v_{\text{target}} \leq v_{\text{ref}}^{1/2}$, the first approximants are the sequence $1/2, 1/3, 1/4, \dots$, and tend to zero slope. In the range $v_{\text{ref}}^{1/2} < v_{\text{target}} < v_{\text{ref}}^{3/2}$, the first approximants are on the partial harmonic fraction, PHF, branches $1 \pm 1/j$. This is the range for the hydrogen constants from the perspective of the proton and the gravitational binding energy. For PHFs if the target lies below the reference, examples include $2/3, 3/4, 4/5, \dots$; if it lies above, the corresponding sequence is $3/2, 4/3, 5/4, 6/5, \dots$. Therefore, the emergence of PHFs in this scalar range is a mathematical imperative of the GON scheme.

If the scalars evaluated are within this range then they do have PHF values. Then they are within a classic resonant physical system, where each PHF is a resonant node. The hydrogen constants' scalars are, therefore, these are within this type of resonant physical structure. This is a potential physical rationale for the origin of this specific structure, but we do not claim clear causality. A trade-off between parsimony and approximation accuracy is inherent: smaller integers tend to have larger possible residuals, and larger denominators tend to have more accurate rational fits [30,31].

Between neighboring rational lattice slopes, the continuous range of numerical values is represented by the residual D_r. For example, the approximate intervals $1/2 \to 1 \to 3/2$, $3/2 \to 2 \to 5/2$, and $5/2 \to 3 \to 7/2$ are continuously interpolated by successive residual values around the corresponding rational slope approximants. In this way, the discrete set of lattice fractions is extended into a continuous scaling space. If the target value remains positive, but is smaller than unity, the same construction applies, with the sign of i or j reversed according to the logarithmic ratio (Figs. 1–3).

The residual D_r therefore measures the displacement from an exact lattice point. Starting from a rational approximant i/j, the residual grows continuously until the midpoint between adjacent approximants is reached, after which the next rational fraction becomes the dominant approximation and the residual changes sign. Repetition of this process generates a piecewise continuous sequence of locally optimal rational approximants, analogous to the progression of continued-fraction convergents in classical Diophantine approximation [30–34].

As the denominator j increases, neighboring rational fractions become more closely spaced, and the typical magnitude of the residual decreases. For the partial harmonic branches, the spacing between adjacent terms scales approximately as $1/j$. Consequently, low-order fractions are

common, but generally admit larger residuals, whereas higher-order fractions provide more accurate approximations at the cost of increased complexity [30,31].

The working hypothesis of this study is that constants as a group exhibit a non-random combination of five features: (i) preference for parsimonious low-order rational PHF exponents, (ii) small residuals D_r, (iii) conformal factors v_{cf} close to unity, (iiii) opposite sign indicate reciprocal numerical relationships, and (iiiii) the constants should be defined by series of small prime factors since these would insure unique numerical orthogonal resonant markers. The low-order is related to parsimony associated with the first fundamental i/j ratio. The j values can be large, and still be the most parsimonious when the ratio of the target and reference are near 1. Such a combination would be statistically restrictive relative to random numerical datasets. We therefore test this expectation explicitly using Monte Carlo methods [51–55]. In this framework, v_{cf} serves as a practical indicator of near-exact scaling for low-order approximants, while recurrent higher-j structure may indicate additional ordered behavior. The specific prime factors are also an important potential non-random characterization.

1.4 First principles motivated by number theory.

The current hypothesis is developed based primarily on mathematics than on dynamical first principles, except that the number system could be resonant one if based on PHFs. It begins with the possibility that fundamental constants, when written as NU frequency scalars, can be organized in a consistent structured mathematical order, by integer fraction power relations, scaling symmetry and geometry utilizing any constant as the reference perspective that exactly define the ratio of one constant to another, therefore, their hierarchy. This perspective is a long tradition in theoretical physics where mathematical regularity has informed physical intuition [19,38,39]. In this type of representation, the constants are compared by ratios of dimensions, and the relative scales of the constants can be analyzed without reference to arbitrary unit choices [16,28,58].

The second assumption is that frequency-based variables offer a natural language comparison of quantities related to mass, length, and energy, as all of them can be related by standard unit conversions in NU systems, just as the Planck scale constants are defined [18,43,44]. In this form, the logarithmic ratios of constants are used to determine scaling exponents which can be studied with rational approximants on an integer lattice as unitized by Minkowski within his GON method. The main question is whether these exponents are randomly distributed or they tend to be concentrated around simple repeating structures.

We use the Hermann Minkowski framework and classical Diophantine approximation [29-34] to explore this possibility since the log ratio of the constants appear to be irrational. The logarithmic exponent of a given reference constant v_{ref} and target constant v_{target} is usually irrational. Rational ratios i/j may be used to approximate this exponent, giving an infinite series of convergents. In the current analysis we consider the most important parsimonious approximant: the smallest irreducible pair (i, j) corresponding to the first local minimum, the fundamental convergence, of the residual D_r as described by Minkowski. The first approximant also generates specific GON properties where the slope is directly related to specific integers linking continuous and rational number systems.

The residual D_r is a measure of the discrepancy between the actual exponent and its rational approximation, and the conformal factor frequency ν_{cf} gives the actual realization in the physical frequency domain and is derived from the ν_{ref}, D_r , i and j. This is to say that D_r and ν_{cf} are not free adjustable fitting parameters, but mathematical measures of departure of the exact rational scaling from a perfect integer power law. Similar concepts, where discrete structures are used to model continuous behavior, are found in number theory, renormalization, and spectral physics [35-37,41].

One of the key organizing principles of the framework is parsimony: out of all the rational approximates that can be constructed, those with the smallest integers and smallest residuals are favored. These minimality conditions are common limiting logical factor in mathematics and theoretical physics, where simple structures are frequently the most general or stable descriptions [27,33,34]. Parsimony links directly to the lattice geometry. In case low-order integer near perfect power law structures are repeated between all constants independent of the reference, then this would be highly statistically constraining compared to random numerical data. We use this method to test the hypothesis on hydrogen as a unified universal electromagnetic gravitational benchmark system since it encompasses the most fundamental forces, energies, and particles. Hydrogen is especially appropriate since its constants are known with great accuracy and its theoretical framework is well developed within the Bohr Model [56,57]. We then enquire whether the mass-force hierarchy which is observed can be described by simple rational power scaling relations, or whether the findings are due to numerical coincidence. This question is assessed explicitly by Monte Carlo comparisons with randomized controls [51-55]. There is no known integer organization of the scale of the constants within the SM so the numerical relationships and their isomorphic forms should be random if analyzed using an integer system. If the scalar system of the constants is highly nonrandom then the hypothesis is supported. Since all of the constants are analyzed as the reference there are 40 degrees of freedom, and no selection bias. In the future more constants could be included.

1.5 Irrational exponents, logarithmic bases, and infinite rational approximants

In modern physics, power laws and discrete quantum numbers are central, and encode hierarchical structure across scales that are widely separated. Scaling relations are found in quantum theory, critical phenomena, and renormalization, and discrete integers are used to label many physical states and symmetry representations [15,27,31,42]. More broadly, exponential and logarithmic mappings give a natural language to compare quantities that vary by many orders of magnitude.

For two positive numbers x and y, the logarithmic ratio $\log(y)/\log(x)$defines the exponent that expresses y as a power of x. If this exponent is irrational, then y cannot be written as an exact integer or rational power of x. This statement is independent of the logarithm base, since changes of base leave the ratio invariant. Although bases such as 10 or e are commonly used, any positive number different from unity may serve as a valid logarithmic base. In the present work, the scalar value of the chosen NU reference constant is used as the base, so that other constants are analyzed relative to its intrinsic scale [16,18,58].

An irrational exponent also implies the existence of an infinite sequence of rational approximates. Through continued fractions and Diophantine approximation, any irrational number admits progressively better rational representations $\frac{i}{j}$ with increasing integer complexity [30–34]. In the present framework, these approximants correspond to an infinite family of isomorphic power-law relations connecting the same pair of constants. In conventional physical applications, one usually retains only the decimal value of the exponent. Here, instead, we examine the associated rational sequence and focus on its leading parsimonious member. This reformulation does not alter the underlying mathematics; rather, it provides an alternative number-theoretic representation of scale relations that may reveal hidden low-order structure not evident in the decimal form alone.

1.6 Paper organization

The rest of this paper will be structured in the following way. Section 2 presents the physical system and the scaling framework. Sec. 2.1 describes the NU frequency representation and Sec. 2.2 explains why hydrogen should be used as a unified electromagnetic-gravitational standard of reference using the Bohr model with gravitational binding added. Section 2.3 elaborates the integer power-law relations based on the Minkowski framework, and the dimensionless lattice formulation (Sec. 2.3.1) and the dimensioned frequency representation (Sec. 2.3.2) are treated separately. The roles of the conformal factor frequency ν_{cf} and the Diophantine residual D_r, are discussed on Sec. 2.4 and the computational search and optimization procedure is described in Sec. 2.5. Sec. 2.6 presents the Monte Carlo methodology of testing departures of random expectations.

Section 3 gives the results, the most significant scaling exponents, the residuals, and conformal factors; the most parsimonious power-law relations; the Monte Carlo significance tests; the hierarchy of electromagnetic and gravitational forces; the prime-factor structure of the most significant approximants; and the higher-order isomorphic rational relations. Section 4 covers the physical interpretation and constraints of the framework. Sec. 5 summarizes final conclusions.

2. Physical System and Scaling Framework

To test any proposed scaling principle meaningfully, a physical system is needed where different regimes of interaction can be compared without making any structural assumptions that are not necessary. Here, we specify the NU representation, the hydrogen benchmark system, and the mathematical framework to explore the possibility of relating electromagnetic and gravitational quantities by parsimonious integer power laws in a single frequency-based description.

2.1 Natural Unit System

To place fundamental constants on a common footing, we express all relevant quantities in equivalent frequency units ν(Hz). We adopt a NU convention in which the speed of light and Planck's constant are set to unity, $c = h = 1$, so that scaling relations are encoded entirely through powers of frequency. This is the unit system of the Planck system. NU formulations of this kind are standard in high-energy and theoretical physics, where dimensional quantities are recast into universal scales [11,18,58]. The reference unit in the present normalization is 1 Hz. Numerical values used throughout this work are taken from the latest NIST CODATA recommendations [18].

The present analysis depends only on ratios of frequencies, and ratio of the logs of the NU frequencies. The framework is effectively dimensionless and independent of any particular time or length scale. In this representation, frequency and wavelength are equivalent descriptions related by inversion, whereas composite units such as eV/c^2 avoidable dimensional structure [16,43,44]. In Number Theory numbers have specific meanings and significance. In this paper the NU scalars hold mathematical significance.

Particle masses conventionally quoted in $\mathrm{eV}/c^2$are converted to frequencies through the energy–frequency relation.

$$\nu = \frac{mc^2}{h} = \xi m, \qquad (4)$$

where

$$\xi = 2.41798935 \times 10^{14} \frac{Hz}{\frac{eV}{c^2}}.$$

This follows directly from the quantum relation $E = h\nu$ together with mass–energy equivalence $E = mc^2$[43,44].

Using this convention, the electromagnetic binding scale of hydrogen, represented by the Rydberg constant R_∞, corresponds to the frequency.

$$\nu_{R_\infty} = cR_\infty = 3.2898421 \times 10^{15}\mathrm{Hz}. \qquad (5)$$

while the proton and electron rest-mass frequencies are

$$\nu_p = 2.26873182 \times 10^{23}\ \mathrm{Hz}, \qquad \nu_e = 1.23559002 \times 10^{20}\ \mathrm{Hz}. \quad (6)$$

These quantities are known experimentally to high precision and form a natural basis for hydrogenic scaling comparisons [11,18,56,57]. Length scales may be written in the same frequency language through $c = \lambda\nu$. The Bohr radius $a_0$is therefore represented by

$$\nu_{a_0} = \frac{c}{a_0}, \quad (7)$$

which gives

$$\nu_{a_0} = 5.66525640 \times 10^{18}\ \mathrm{Hz}. \qquad (8)$$

The Bohr radius and Rydberg scale are central parameters of the hydrogen atom and encode its characteristic spatial and energetic structure [56,57].

The gravitational binding energy of the electron in hydrogen is given by,

$$E_{\mathrm{GBE,e}} = \frac{Gm_p m_e}{a_0}, \qquad (9)$$

which may be written as an equivalent frequency through division by Planck's constant,

$$\nu_{\mathrm{GBE},e} = \frac{E_{\mathrm{GBE.e}}}{h} = \frac{G m_p m_e}{a_0 h}, \qquad (10)$$

Substituting the standard values of the constants [18] gives

$$\nu_{\mathrm{GBE},e} \approx 2.90025 \times 10^{-24}\ \mathrm{Hz}. \qquad (11)$$

For later comparison, the reciprocal proton frequency is

$$\nu_p^{-1} = 4.407748824 \times 10^{-24}.$$

The numerical proximity between $\nu_{\mathrm{GBE},e}$ and ν_p^{-1} motivates the scaling analysis developed in the following sections. Whether this correspondence reflects underlying structure or numerical coincidence is tested quantitatively using the lattice and Monte Carlo methods introduced later [29–34,51–55]. There is a valid criticism that the gravitational binding energy is not directly measurable, but it is an accurate value. This same criteria is also a valid criticism of the rest mass of the electron, the Bohr radius, and the R_∞ , but these are all well-established valid constants so we utilize them.

2.2 Choice of Unified Physical System: Electromagnetic and Gravitational Binding in the Bohr Model

We adopt the hydrogen atom as the benchmark system, using the ionization-energy scale R_∞(the Rydberg constant) as the reference quantity. Particular attention is given to the proton p, electron e, Bohr radius a_0, and the gravitational binding energy of the electron in hydrogen, $E_{\mathrm{GBE},e}$. Hydrogen is especially suitable because it is a closed, and analytically tractable system whose characteristic scales are determined by well-known masses, geometry, and fundamental constants [56,57]. It encompasses many of the most fundamental forces (electromagnetic, and gravitational), energies (ionization), and particle masses (strong and weak). We also analyze all of the other constants as the reference, but focus on these two since it is a direct scaling of the ratio of the electromagnetic forces to gravity within the same system.

Its electromagnetic structure is described with high precision, historically through the Niels Bohr model and later generally through quantum mechanics [56,57]. The same particle masses and orbital radius that determine the electromagnetic binding energy also define the corresponding gravitational binding energy, differing only by the interaction coupling.

Although $E_{\mathrm{GBE},e}$is extremely small and not directly measurable, it is a well-defined derived quantity constructed from accepted constants. This allows electromagnetic and gravitational binding scales to be compared within a single internally consistent framework. Hydrogen therefore provides a clean testbed for assessing whether the proposed scaling relations reflect genuine inter-force structure or numerical coincidence [18,51–55].

2.3 Quantum Parsimony Diophantine Resonance Power Laws Between Two Constants

In this section, we outline the dimensionless and dimensioned forms of the lattice framework used in this work, together with the basic assumptions underlying the proposed power-law relations between pairs of constants.

2.3.1 The Dimensionless Domain

The construction is entirely number theoretic in the dimensionless Minkowski domain and does not rely on any physical interpretation. This is an advantage since it does not add any new physics, and is well known. Two positive scalar frequencies are assigned as a reference quantity $[\nu_{\mathrm{ref}}]$, a target quantity $[\nu_{\mathrm{target}}]$, and brackets are used to represent dimensionless numerical scalar values. The logarithmic ratio is the exact scaling exponent between the two quantities.

$$\mathrm{slope}(\mathrm{ref{:}\,target}) = \exp(\mathrm{ref{:}\,target}) = \frac{\log([\nu_{\mathrm{target}}])}{\log([\nu_{\mathrm{ref}}])} = \frac{\log([\nu_{\mathrm{target}}/\nu_{\mathrm{ref}}])}{\log([\nu_{\mathrm{ref}}])} + 1. \qquad (12)$$

Since the logarithmic ratios do not change with the change of base, the exponent is only dependent on the relative magnitudes of the two numbers, but not the logarithm convention used. The slope could be defined using natural log, as well, with no changes in the ratio.

In the case where this exponent is irrational, it can be approximated by a rational power i/j, i and j being integers. The difference between the rational approximation and the actual exponent is measured by the Diophantine residual.

$$D_r = \exp(\mathrm{ref{:}\,target}) - \frac{i}{j}, \qquad (13)$$

that quantifies the quality of the approximation in the standard sense of Diophantine analysis [29-34]. The pair (i, j) of orders is an integer point on the lattice $\mathbb{Z}^2$ Figure (1,2,6).

Admissible approximants are only taken to be rational pairs i/j that give local minima of $|\ D_r\ |$. These are geometrically the points where the line specified by the exact exponent is closest to successive lattice points. This picks out a sparse and ordered infinite set of all possible integer pairs and leaves out the vast majority of the lattice points.

The admissible pairs are obtained in a series as the lattice search is extended to larger integer domains. Every valid approximant is thus identified by an order label #1,#2,#3,... along with its associated i/j , residual D_r and derived power-law relation. In the current work, special attention is paid to the first and the most parsimonious in this infinite series. The first is the only unique one.

Figure 6. Geometry of first rational approximants, convergences, on the Minkowski lattice for the $(R_\infty\mathrm{:\,GBE}_e)$system.

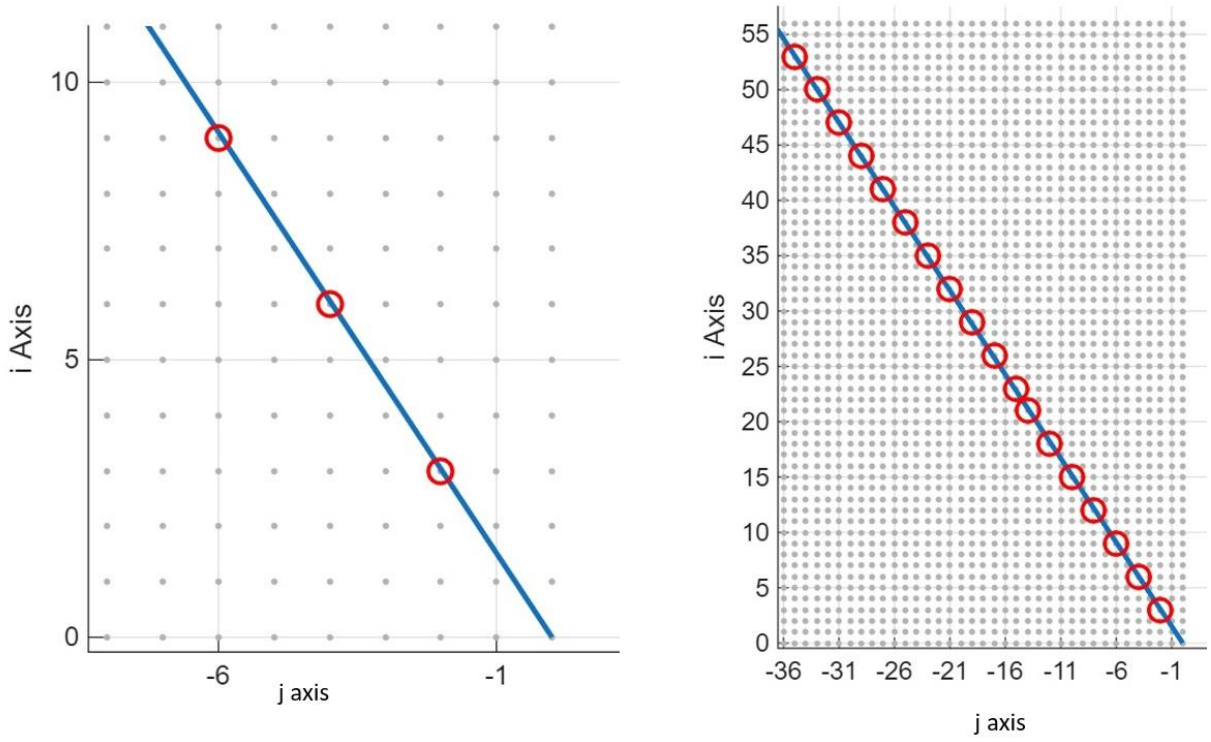

Figure 6 shows the GON, construction of the pair $(R_\infty, \mathrm{GBE}_e)$, with the horizontal axis the denominator j, of the integer and the vertical axis the numerator i. The blue line is the precise logarithmic exponent of the two quantities, whose numerical slope is approximately -1.51687, and is near the rational number $-3/2$.

Red circles denote lattice points that are related to local minima of the Diophantine residual $|D_r|$. These points are successive admissible rational approximates and the respective candidate power-law relations. The left panel gives a "zoomed-in" view of the lowest-order region, with the leading approximants being $-3/2$, $-6/4$, and $-9/6$; the irreducible form $-3/2$, is chosen as the parsimonious representative.

The right panel depicts the larger lattice structure at larger integer values where more convergences are observed along the same line. The points on the opposite sides of the precise exponent line are associated with the alternating signs of the residual D_r, and the size of the residual tends to be smaller with larger integers. This is a sequence of convergences in order which is typical of fractal classical rational approximation on integer lattices [29-34]. Similar GON could be generated for every possible constant pair.

2.3.2 The Dimensioned Frequency Domain

We now introduce the realization of the scaling architecture in the dimensioned physical domain, having first established its form in the dimensionless lattice domain. This extension is not part of the classical Minkowski construction itself, but is introduced here to connect the discrete integer-power representation on the $\mathbb{Z}^2$ lattice with measurable physical frequencies. In this framework, the conformal factor frequency ν_{cf} provides the link between the dimensionless lattice description and the continuous physical domain.

The quantity ν_{cf} is defined as a function of the Diophantine residual D_r, and is therefore not an external fitting parameter. Dividing ν_{target} and ν_{ref} by ν_{cf} maps the corresponding quantities to dimensionless scalars that align perfectly with the $\mathbb{Z}^2$ lattice, while multiplication by ν_{cf} returns the lattice values to the physical frequency domain. In this sense, ν_{cf} acts as the dimensional realization of the residual structure and provides the connection between rational dimensionless lattice exponents; and irrational dimensioned physical scales, and irrational powers. The transformation factor may be written equivalently in terms of the residual or the integer powers as

$$\nu_{cf}(\text{ref: target}, i/j)\ \text{Hz} = \nu_{\text{ref}}^{D_r\, j/(j-i)}\ \text{Hz} = \left(\frac{\nu_{\text{target}}^{j}}{\nu_{\text{ref}}^{i}}\right)^{1/(j-i)}\ \text{Hz}, \qquad (14)$$

which shows that ν_{cf} is determined directly by the intrinsic scale relation between the two constants. The full set of admissible rational approximants generates a structured three dimensional manifold in the space of D_r and ν_{cf}. The corresponding D_r values define a discrete Diophantine spectrum associated with successive lattice convergences. This spectrum is not a wave function, but rather a structured sequence of residuals arising from the approximation of irrational exponents by rational lattice points. The dimensioned scaling relation between ν_{target}, ν_{ref}, and ν_{cf} is then written as

$$\nu_{\text{target}}\ \text{Hz} = \nu_{cf}\left(\text{ref: target}, \frac{i}{j}, \#n\right)^{1-(i/j)}\ \nu_{\text{ref}}^{\,i/j}\ \text{Hz}, \qquad (15)$$

so that ν_{target} is expressed as the product of ν_{cf} raised to the power $1 - i/j$ and ν_{ref} raised to the power i/j. If the ν_{cf} equals 1 Hz then the power law is perfect and the D_r equals 0. The closer ν_{cf} is to 1 Hz the "more" perfect the power law is. In the SM there is no reason why the constants' power laws should be near perfect.

2.3.3 Dimensionless relations for $\nu_{\text{ref}}/\nu_{\text{target}}$, ν_{cf}, and mass–force hierarchy power laws

The ratios $\nu_{\text{ref}}/\nu_{\text{target}}$ define exact dimensionless power-law relations in terms of ν_{ref}, ν_{target}, i, j, and ν_{cf}. These relations provide the basis for the definition of hierarchy scaling examined in this work. When ν_{cf} is divided into both ν_{ref} and ν_{target}, the resulting quantities become dimensionless and preserve the invariant rational exponent $i, j\ and\ i/j$, independent of the choice of units. U represents a variable unit scalar factor. It would have no effect on the powers. The basic relations are

$$\frac{U\nu_{\text{ref}}}{U\nu_{\text{target}}} = \left[\frac{U\nu_{\text{ref}}}{U\nu_{cf}(\text{ref: target}, i/j)}\right]^{(j-i)/j} = \left[\frac{U\nu_{\text{target}}}{U\nu_{cf}(\text{ref: target}, i/j)}\right]^{(j-i)/i}, \qquad (16)$$

$$\frac{\nu_{\text{target}}}{\nu_{cf}(\text{ref: target}, i/j)} = \left[\frac{\nu_{\text{ref}}}{\nu_{cf}(\text{ref: target}, i/j)}\right]^{i/j}, \qquad (17)$$

and

$$\left[\frac{\nu_{\text{target}}}{\nu_{cf}(\text{ref: target}, i/j)}\right]^{j/i} = \frac{\nu_{\text{ref}}}{\nu_{cf}(\text{ref: target}, i/j)}. \qquad (18)$$

These relations show that the hierarchy between two constants may be written within two different power laws using the same i, j values in a different algebraic power forms entirely in terms of dimensionless power laws defined by the one constant and a common v_{cf} in isolation. In this way, the power laws play a role analogous to scaling constants, but without introducing additional external physical parameters.

2.4 Computational Search and Optimization Criteria

We systematically search the expanding integer lattice $\mathbb{Z}^2$ with MATLAB and Excel spreadsheet-based implementations to identify the integer power-law relations of the proposed scaling framework. The algorithm scans pairs of consecutive increasing integers (i, j) within a two dimensional array and finds those pairs that are related to local minima of the absolute Diophantine residual in Eq. (13). These locally optimal pairs are the only admissible rational approximants.

The main optimization criterion applied to determine the hierarchy is parsimony. Of all admissible integer ratios, the smallest irreducible pair that first appears in the ordered search sequence ($n = \#1$) is preferred where the residual is as close to a local minimum as possible. Even though there are infinitely many higher-order approximants, the first admissible pair is considered to define the leading hierarchy relation since it is linked to the GON. To achieve numerical stability and visualization, the search is carried out by the reciprocal residual

$$\frac{1}{\mid \exp(\text{ref: target}) - \frac{i}{j} \mid} = \frac{1}{\mid D_r \mid} \to \infty, \qquad (19)$$

accessed in pairs of irreducible integers (i, j). Maxima of Eq. (19) are identical to minima of $\mid D_r \mid$, and candidate solutions can be found efficiently. In this representation, the higher the peaks, the more precise the rational approximants. An Excel and MATLAB script were both utilized for the calculations. The program finds the emergent powers, D_r, and v_{cf} values. They are not fit.

The higher-order resonances with larger integer pairs are also noted, as they produce an infinite hierarchy of further power-law solutions. Every admissible pair is associated with its v_{cf}, residual D_r and order label n#. These long-term solutions are studied by tabulated outcomes and graphical representations of the residual landscape.

The most parsimonious approximants are highlighted in the current study along with the corresponding i/j, D_r and v_{cf} values. We summate the normalized v_{cf} , if less than 1 then the reciprocal, values for each reference to evaluate how close they are to perfect power laws. We also investigate lattice degeneracies, prime-factor structure, higher-order resonances, and continued-fraction properties of the resulting exponents to determine whether the observed hierarchy is consistent with random expectations or a more ordered numerical pattern [29-34,51-55].

2.5 Monte Carlo simulations

We created a series of Monte Carlo simulations using MATLAB to evaluate what are the characteristics of the i/j, D_r, and v_{cf} values of a pair of constants and an ensemble of random

numbers utilized within this mathematical framework. This creates a null hypothesis that can be tested against the known constants properties.

Figure 4. Monte Carlo baseline probabilities for first-order rational approximants i/j.

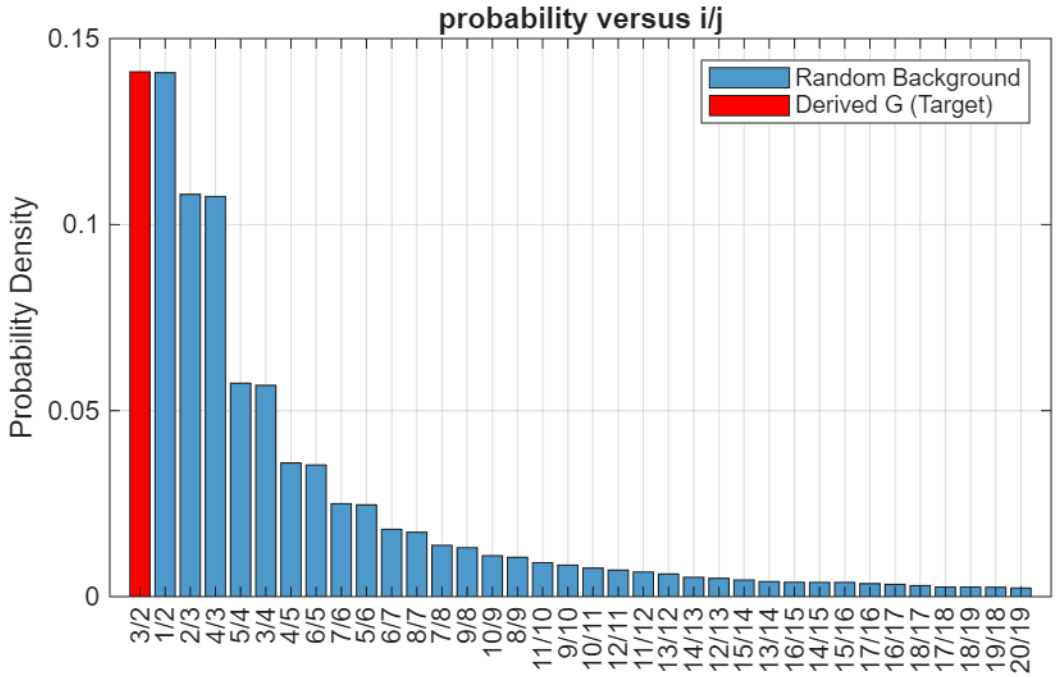

Figure 4 illustrates the probability distribution y-axis of denominator values i/j x-axis of leading rational approximants of 10^6 Monte Carlo trials with randomly sampled target frequencies in the range $10^{6.8}$ to 10^{24}, with v_{R_∞} as the reference scale. This is approximately from $v_{ref}{}^{1/2}$ to $v_{ref}{}^{3/2}$.

The blue bars are the empirical Monte Carlo frequencies of the random ensemble. The red bar indicates the case of hydrogen gravitational binding-energy and R∞ as the reference, the leading approximant of which is $|-\frac{3}{2}|$ [30,33]. As the j increased the probability drops with approximately a value of $1/j^2$.

This distribution indicates that low-denominator fractions are highly preferred in random datasets, with approximants of larger j occur becoming less frequent in random datasets. So, the occurrence of a small denominator like $j = 2 - 7$ is not in itself an indication of non-random structure. Instead, statistical significance should be evaluated together with other requirements, including the size of the residuals, consistency of patterns among various constants, and the corresponding v_{cf} values.

Figure 5. Random v_{cf} spectrum for the (R_{∞}, corresponding random targets) pair and the observed values.

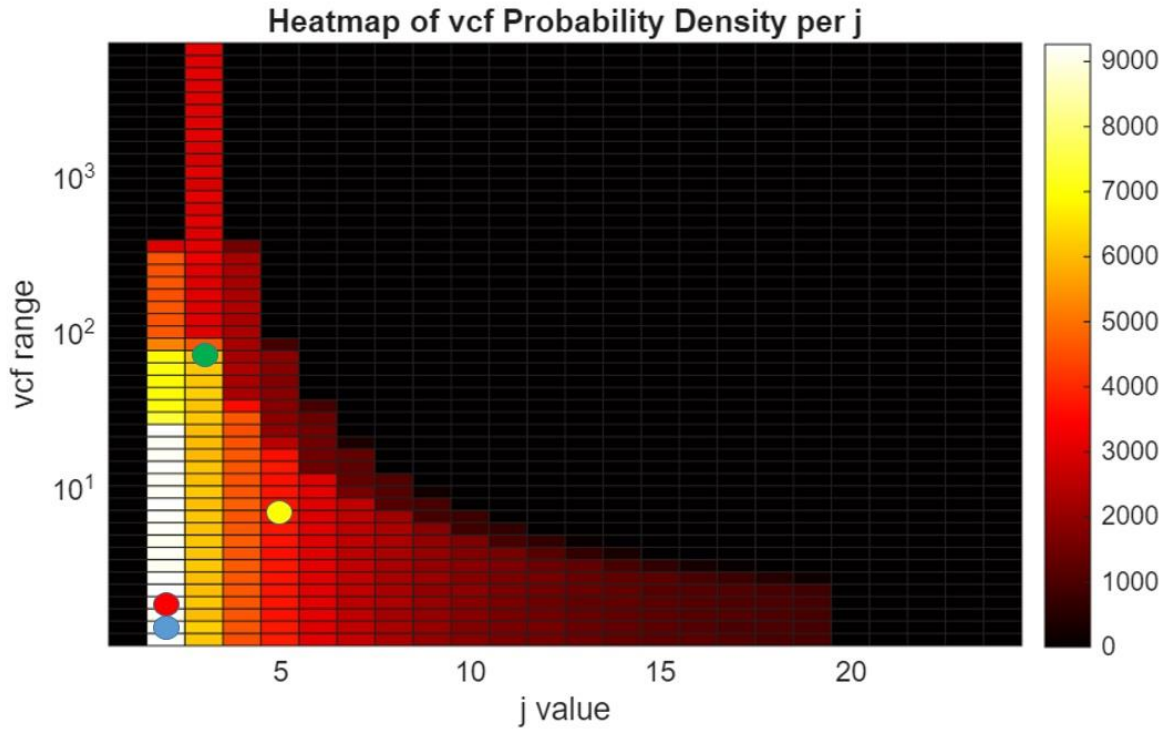

Figure (5) is a graph of the v_{cf} spectrum for the R_{∞} as the reference versus 1 million iterations of random target values. The observed v_{cf} values for this group of constants are shown. A Monte Carlo series was generated with a range of $10^{6.8}$ to 10^{24} which generates symmetric values for either 3/2 or 1//2. The probabilities of the v_{cf} were collated versus the j value. The color is a "heat map" of the likelihood of any specific v_{cf} for each j. It demonstrates that in general the lower the j the larger the ranges of possible v_{cf} values, and they are more common. The likelihood of a specific v_{cf} value for each j is quite broad. The higher the j the lower the v_{cf} values in scale, and less likely the probability. The blue circle is for GBE, red for the proton, green for the electron, and yellow for the Bohr radius. The v_{cf} values for R_{∞}:$GBE,_e$ and R_{∞}:p are both demonstrating non-random characteristics as v_{cf} values near 1 for small j values. The others are random.

Figure (6) probability of the product of four v_{cf} values for a random five constant reference and target system

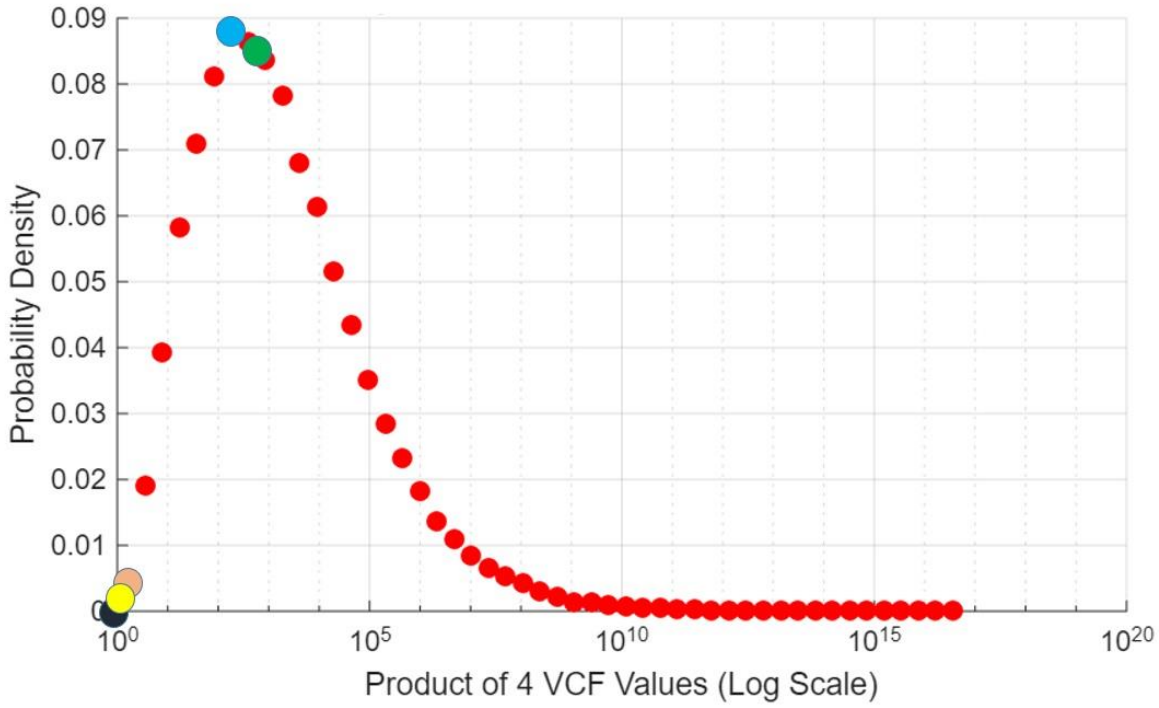

Figure (6) is a Monte Carlo simulation where five random values from a range of 10^{14} to 10^{24} are selected randomly. One is randomly chosen as the reference. The four i, four j, four v_{cf}, four D_r values were derived and collated for each iteration of one million. The product of the four v_{cf} is a measure of the global alignment of a five constant system is to four perfect power laws. The lower the product the more perfect the power law system. The probability of the specific product of the v_{cf} values is plotted. The graph is a skewed probability pattern where the most likely values in the range of $10^{2.5}$ or 300. There is a sharp drop off as the product decreases with rare values below 10. There is a long tail drop off as the values increase above 10^6. The black circle is the for four v_{cf} product for $GBE,_e$ as the reference, yellow for the proton, tan for a_0, blue for e, and green for R_∞. The probabilities for the v_{cf} products for $GBE,_e$ and the p are rare, while e and R_∞ are more random.

Figure (7) probability of the maximum j of four v_{cf} values for a random five constant reference and target system

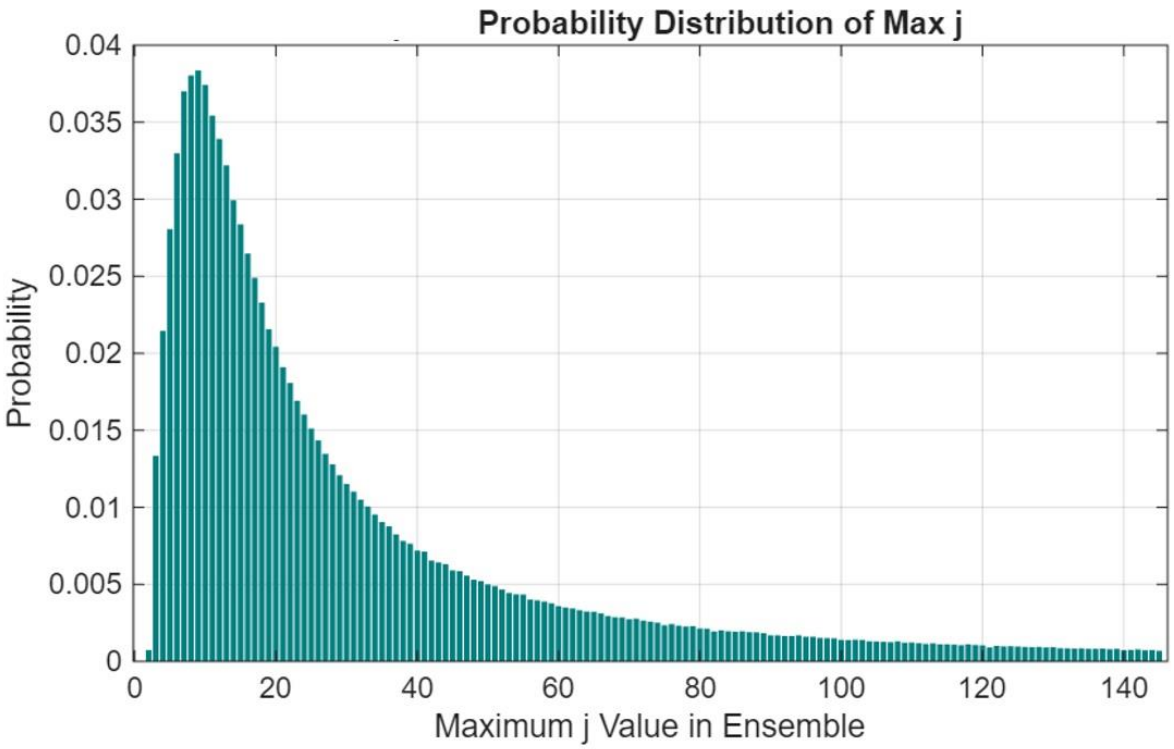

Figure (7) is a Monte Carlo simulation where five random values from a range of 10^{14} to 10^{24} are selected randomly. One is randomly chosen as the reference. The four i, four j, four v_{cf}, four D_r values were derived and collated. The maximum j of each ensemble of the four target random values, x-axis, was collated and plotted as probabilities, y-axis. Since the known constants are composed of values where the reciprocal of one is nearly equal to the other in this Monte Carlo simulation the equivalent is randomly encountering two random values that are nearly identical. This is only associated when the j value is high. The most common maximum j values are in the range of 5 to 15. The likelihood of randomly encountering a high max j value drops off in a long tail to the right. The likelihood for a j max in the range of 129 is approximately 1 in one thousand. The j values for GBE, and the p are in this range so they are rare.

Therefore the product of the known four vcf values and the maximum j for $GBE_{,e}$ and the p as the references are both the exact opposite of what a random system would produce [30-34]. This is not true for the other constants as potential references. Therefore these two are the constants that should be utilized as the reference values.

3. Results

This part shows the quantitative findings of the implementation of the Minkowski approximation framework, Eqs. (2) and (11)-(15), with R_∞ as the reference scale and a_0, e, p, and GBE_e as desired quantities in the hydrogen system. The $(R_\infty, \mathrm{GBE}_e)$ pair is given special attention, as it offers the strongest electromagnetic-gravitational hierarchy and demonstrates the entire framework of the approach. We evaluate all of the constants a reference values in an identical fashion as well, but only the data from that set will be shown as charts since it is to exhaustive.

The findings are presented in Tables (1-10) and related figures. These are the most important rational approximants i/j, the exact logarithmic slopes, the residuals D_r, the conformal factors v_{cf}, the equivalent power-law forms, the higher-order resonances, and the statistical comparisons with randomized ensembles. We also discuss the prime-factor structure of the dominant exponents and the degeneracy pattern of equivalent lattice representations.

3.1 Leading i/j, slopes, exponents, and $\nu_{\mathrm{ref}}/\nu_{\mathrm{target}}$ power laws

The Tables list the first admissible approximant (#1) for each target constant, together with the exact slope exponent, the ratio $\nu_{\mathrm{ref}}/\nu_{\mathrm{target}}$, and the associated dimensionless scaling relation derived from Eqs. (16)–(18). In each case, the exact logarithmic slope lies close to a simple low-order rational number.

Table (1): Leading first-order Minkowski approximants for hydrogen referenced to R_∞, listing i/j, exact slope exponents, ratios $\nu_{\mathrm{ref}}/\nu_{\mathrm{target}}$, and the corresponding dimensionless power-law forms.

constant	i/j (#1) decimal	slope , exponent	ν_{ref}/ν_{target}	$\left[\frac{\nu_{ref}}{\nu_{cf}\left(ref:target,-\frac{i}{j}\right)}\right]^{(j-i)/j}$
GBE, e	-3/2 -1.5	-1.51687	1.134331 10^{39}	$\left[\frac{\nu_{RH}}{\nu_{cf}\left(RH:GBEe,-\frac{3}{2}\right)}\right]^{5/2}$
R_∞	1	1	1	
a_0	6/5 1.2	1.208545982	5.807048910 10^{-4}	$\left[\frac{\nu_{RH}}{\nu_{cf}\left(RH:a_0,\frac{6}{5}\right)}\right]^{-1/5}$
e	4/3 1.333333	1.294815217	2.66256772 10^{-5}	$\left[\frac{\nu_{RH}}{\nu_{cf}\left(RH:e,\frac{4}{3}\right)}\right]^{-1/3}$
p	3/2 1.5	1.505156904	1.450079766 10^{-8}	$\left[\frac{\nu_{RH}}{\nu_{cf}\left(RH:p,\frac{3}{2}\right)}\right]^{-1/2}$

For the hydrogen system referenced to R_∞, the leading exponents are found to be $-3/2$ for GBE_e, 1for R_∞, $6/5$ for a_0, $4/3$ for e, and $3/2$ for p. With the exception of the identity case, these values belong to the partial harmonic fraction family $1 \pm 1/j$, consistent with the scale interval identified in Sec. 2, Fig (1,2,6). The observed constants therefore occupy a sparse subset of the admissible low-order rational positions defined by the prime factors 2, 3, and 5. These results show that the

ratios $\nu_{\mathrm{ref}}/\nu_{\mathrm{target}}$ can be represented by compact power-law forms involving only ν_{ref}, ν_{cf}, and small integer exponents. In this sense, ν_{cf} acts as the scale factor that completes the mapping between the exact physical ratios and their parsimonious lattice approximants.

3.2 Geometry -of -Number line plots of the constants

Figure 7 presents Geometry of Numbers, GON, lattice plots for the principal hydrogen constants referenced to R_∞. In each panel, the horizontal axis denotes the integer denominator j, while the vertical axis denotes the numerator i, over the range $1 \le i, j \le 100$(with negative $j$included for the $(R_\infty : \mathrm{GBE}_e)$case). The plotted systems correspond to $(R_\infty : \mathrm{GBE}_e, -3/2)$, $(R_\infty : p, 3/2)$, $(R_\infty : a_0, 6/5)$, and $(R_\infty : e, 4/3)$.

Figure (7): Geometry of the numbers plots for the five constant ensemble for the $R\infty$ as the reference

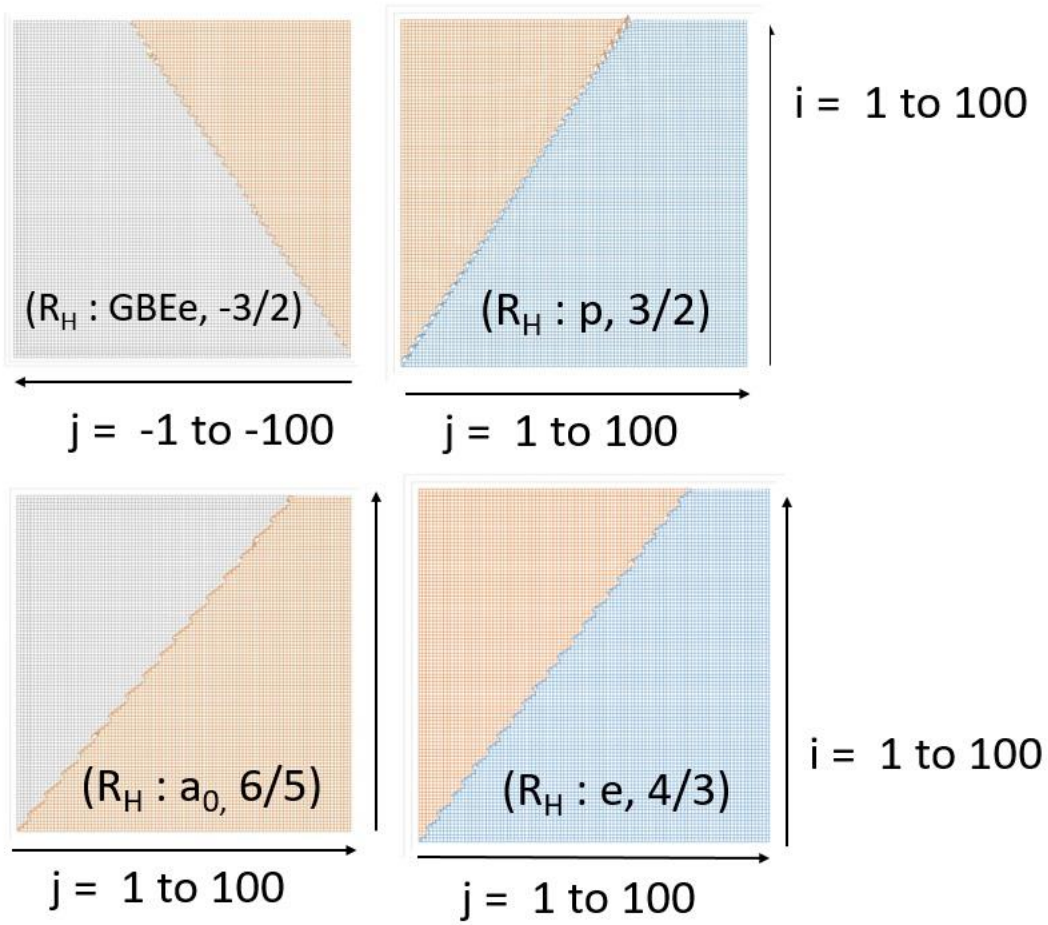

Figure 7. The zig-zag thin boundary between the two-colored areas determines the series of locally optimal lattice convergences of each exponent. This line is the admissible rational approximants of the Diophantine search process outlined on Sec. 2.4. The points that are closest to the true slope have smaller residuals and thus more precise power-law models.
The upper-left and upper-right panels are a mirror pair of the negative and positive $3/2$ branches, and the lower panels show the adjacent partial harmonic fractions $6/5$ and $4/3$. These branches

approach the unit slope more and more as the integers get larger, which is also in line with the partial harmonic fraction sequence mentioned above.

Figure 7 thus shows how the chosen hydrogen constants fill separate low-order sectors of a shared lattice structure, instead of being represented as isolated numerical coincidences. This parallels the results seen in Fig. (1,2).

3.3 i/j, PHF, D_r, v_{cf}

Table 2 lists the first admissible approximants (#1) of the hydrogen benchmark system, along with their partial harmonic fraction (PHF) forms, D_r, and conformal factor frequencies v_{cf}. The PHF representation is based on the order $1 \pm (1/j)$ that defines the dominant branch that is known to be used in the scale interval of interest.

Table (2): First-order Minkowski approximants for hydrogen referenced to R_∞: leading i/j, PHF forms, D_r, v_{cf}

Constant pair	i/j {2,3,5}	D_r	v_{cf}
R_∞:GBE	-3/2	$-1.68718\ 10^{-2}$	$7.857405\ 10^{-1}$
R_∞:R_∞	1		
R_∞:a_0	6/5, (2·3)/(5)	$8.545984443\ 10^{-3}$	$2.172462647\ 10^{-1}$
R_∞:e	4/3, $2^2/3$	$-3.851811505\ 10^{-2}$	$6.209791219\ 10^{1}$
R_∞:p	3/2	$5.156906446\ 10^{-3}$	$6.917652790\ 10^{-1}$

The product of the four v_{cf} values is global measure of how near perfect the ensemble of constants are all to true power laws. The product of the four normalized v_{cf} values for this group is 525.88. If v_{cf} was less than 1 then 1/ v_{cf} was utilized.

The leading exponents are $-3/2$ for GBE_e, 1 for R_∞, $6/5$ for a_0, $4/3$ for e, and $3/2$ for p.. These values are simple low-order rational numbers constructed out of the first 3 prime factor integers, and the intermediate fraction $5/4$ is represented by an admissible lattice position not taken up by one of the chosen constants.

The conformal factors v_{cf} fix the dimensional correction needed to scale the rational lattice approximation to the physical value. Values of v_{cf} near unity are particularly close realizations of the suggested power-law form, and larger or smaller values are stronger rescaling. In the positive hydrogen branch (a_0, e, p), the denominators are decreasing in the following order of the first three prime numbers $\{5,3,2\}$, i.e. $6/5$, $4/3$, and $3/2$. This development indicates the systematic arrangement of the constants in the partial harmonic branch instead of arbitrary arrangement. In the current analysis, v_{cf} is was taken as a convenient measure of parsimony since it is more sensitive than D_r alone to near-exact scaling relations.

Table (3): First-order Minkowski approximants for hydrogen referenced to p: leading i/j, PHF forms, D_r, v_{cf}

Constant pair	i/j {2,3,5,7,43}	D_r	v_{cf}
p:GBE	-129/128 $-(3\cdot43)/2^8$	$2.93529\ 10^{-5}$	1.000787
p:R_∞	2/3	$-2.28410581\ 10^{-3}$	$6.917652790\ 10^{-1}$
p:a_0	4/5, $2^2/5$	$2.936876061\ 10^{-3}$	2.202749961
p:e	6/7, (2·3)/7	$3.109793421\ 10^{-3}$	3.224197417
p:p	1/1		

The product of the four normalized v_{cf} values for this group is 10.275.

Table (4): First-order Minkowski approximants for hydrogen referenced to GBE_e: leading i/j, PHF forms, $D_r,\ v_{\mathrm{cf}}$

Constant pair	i/j {2,3,5,7,43}	D_r	v_{cf}
GBE:GBE	1		
GBE:R_∞	-2/3	$7.415157251\ 10^{-3}$	$7.857405274\ 10^{-1}$
GBE:a_0	-4/5, $-2^2/5$	$3.264235558\ 10^{-3}$	$9.063907592\ 10^{-1}$
GBE:e	-6/7, -(2·3)/7	$3.533970075\ 10^{-3}$	$9.020076157\ 10^{-1}$
GBE:p	-128/129 $-2^8/(3\cdot43)$	$-2.276962\ 10^{-3}$	1.000787

The product of the four normalized v_{cf} values for this group is 1.5579.

Table (5): First-order Minkowski approximants for hydrogen referenced to a_0: leading i/j, PHF forms, $D_r,\ v_{\mathrm{cf}}$

Constant pair	i/j {2,3,5,7}	D_r	v_{cf}
a_0:GBE	-5/4, $-5/2^2$	$-5.12126\ 10^{-3}$	$9.06391\ 10^{-1}$
a_0:R_∞	5/6, 5/(2·3)	$-5.892745327\ 10^{-3}$	$2.172462647\ 10^{-1}$
a_0:a_0	1		

a_0:e	15/14, (3·5)/(2·7)	-4.590585244 10^{-5}	1.028140236
a_0:p	5/4, $5/2^2$	-4.572084289 10^{-3}	2.202749961

The product of the four normalized v_{cf} values for this group is 11.501.

Table (6): First-order Minkowski approximants for hydrogen referenced to e: leading i/j, PHF forms, D_r, v_{cf}, and Monte Carlo results

Constant pair	i/j {2,3,5,7}	D_r	v_{cf}
e:GBE	-7/6, -7/(2·3)	-4.830040022E-03	9.020076157 10^{-1}
e:R_∞	¾, $3/2^2$	2.231097216E-02	6.209791219 10^{1}
e:a_0	14/15, (2·7)/(3·5)	3.999081155E-05	1.028140236
e:e	1/1		
e:p	7/6, 7/(2·3)	-4.217472997E-03	3.224197417

The product of the four normalized v_{cf} values for this group is 228.21.

Overall, the Monte Carlo tests indicate that the low-order rational structure observed for the hydrogen constants is highly statistically unusual. This finding does not prove physical causality, but it is consistent with the pattern being more structured than would be expected from random sampling for the proton and $GBE_{,e}$ as the reference values.

3.4 Lattice-grid degeneracies and the i/jmass–force hierarchy

Table 7 shows a finite subset of the Minkowski lattice $\mathbb{Z}^2$ in terms of the integer coordinates (i, j) of first-order rational approximants. The dimensioned relations are mapped back onto the lattice points when the physical target and reference frequencies are scaled by their respective v_{cf} values, which is equivalent to stripping the residual D_r from the irrational exponent representation [Eqs. (12), (16)–(18)]. Thus, the continuous physical scaling relations are mapped onto rational coordinates.

Table 7. Finite section of the Minkowski lattice $\mathbb{Z}^2$showing rational i/jcoordinates and the locations of the principal hydrogen constants referenced to R_∞: $\mathrm{GBE}_e = -3/2, p = 3/2, e = 4/3$, $a_0 = 6/5$, and $R_\infty = 1$.

-6/6	-6/5	-3/2	-2	-3	6	6	3	2	3/2	6/5, a_0	6/6
-5/6	-5/5	-5/4	-5/3	-5/2	5	5	5/2	5/3	5/4	5/5	5/6
-3/4	-4/5	-4/4	-4/3	-2	4	4	2	4/3, e	4/4	4/5	3/4

-1/2	-3/5	-3/4	-3/3	-3/2, *GBE,e*	3	3	3/2, *p*	3/3	3/4	3/5	1/2
-1/3	-2/5	-1/2	-2/3	-2/2	2	2	2/2	2/3	1/2	2/5	1/3
-1/6	-1/5	-1/4	-1/3	-1/2	-1, $1/R_\infty$	1, R_∞	1/2	1/3	1/4	1/5	1/6
-6	-5	-4	-3	-2	-1	1	2	3	4	5	6

The table shows all of the i, j matrix locations of the lattice. There is degeneracy of the lattice. There are many different integer pairs that represent the same rational number, for example, $3/2$, $6/4$, and $9/6$, all represent the same slope, Fig, (1,2). In the current work, these degeneracies are collapsed to their irreducible forms, with the smallest pair being the parsimonious form. This lattice was utilized to search for the most parsimonious i/j pair for each constant pair.

The hydrogen constants are located at a few of the lattice points. The gravitational binding energy GBE_e and proton branch are at $-3/2$ and $3/2$, respectively. The electron is at 4/3, the Bohr radius at 6/5 and the identity R_∞ at unity as the reference. All these are members of the partial harmonic fraction sequence. So, an infinite number of possible rational lattice points, for the chosen hydrogen system, reduces to a small, ordered set of low-order fractions. Table 3 illustrates this proposed mass–force hierarchy in the lattice. A similar grid could be created for each reference constant.

3.5 The prime factor grid mass force hierarchy and Number Theory logic

Table 8 is a re-arrangement of the leading rational exponents i/j by prime factors. Since every rational number can be uniquely expressed as a product of prime factors, this is another arithmetic perspective on the hierarchy of the hydrogen scaling relations. If the constants are structured by numbers then primes are essential to avoid degeneracy and resonance interference.

Table 8. Prime-factor decomposition of the dominant first-order Minkowski approximants for the hydrogen system, revealing how the dominant exponents $-3/2$, 1, $6/5$, $4/3$, and $3/2$ are built from the small primes $\{2, 3, 5\}$.

system {prime factors} ={2,3,5}	i/j (#1)	1	2	3	5
GBE, e {2,3} sign inversion	-3/2		2	-3	
R_∞ {}	1	1			
a_0 {2,3,5} closest to 1	6/5		2	3	5
not the most parsimonious, does not exist	5/4		2^2		5
e {2,3} next closest to 1	4/3		2^2	3	
p {2,3} least close to 1	3/2		2	3	

For the leading constants of hydrogen, the dominant exponents are constructed from the low primes $\{2, 3, 5\}$: $-3/2$ for GBE_e, 1 for R_∞, $6/5$, $4/3$, and $3/2$. The Bohr-radius branch thus has the product 2×3 in the numerator and 5 in the denominator, while the electron and proton

branches are built from the small primes 2 and 3. The minus sign of $-3/2$ is due to inversion with respect to the reference branch.

This arrangement shows two aspects of the parsimonious solutions. First, the hierarchy is represented by low-order integers with minimal prime complexity and powers. Second, as the rational exponents converge to unity, larger composite numerators and denominators emerge, in line with the partial harmonic fraction sequence. The intermediate fraction 5/4, while mathematically possible, is not chosen by one of the hydrogen constants. This shows that not all low-order lattice fractions are occupied in the current system. Table 4 thus demonstrates that the scaling relations identified can be represented not only geometrically on the lattice, but also arithmetically by a small number of prime factors with parsimony defining what is possible. Similar grids could be made for each reference.

For the R_∞ reference only the prime set of {2,3,5}. The e and a_0 references are defined by the prime set of {2,3,5,7}. The GBE and p references are defined by the prime set of {2,3,5,7,43}. The distribution of primes in each reference set could be random, but the results suggest order.

3.6 Electromagnetic–gravitational force hierarchy ratio

A direct consequence of the power-law construction is an exact representation of the ratio between the electromagnetic and gravitational binding scales in the hydrogen system. This ratio is central to the present analysis because it captures, within a single benchmark, the large disparity between the two interaction strengths. This same approach could be utilized for any two constants.

The ratio of the corresponding frequencies is

$$\frac{\nu_{R_H}}{\nu_{GBE_e}} = 1.13433 \times 10^{39}. \qquad (20)$$

Using Eq. (16), the same quantity may be written in equivalent power-law form as

$$\frac{\nu_{R_H}}{\nu_{GBE_e}} = \left[\frac{\nu_{R_H}}{\nu_{cf}(RH{:}\,GBE_e, -3/2, \#1)}\right]^{5/2} = \left[\frac{\nu_{GBE_e}}{\nu_{cf}(RH{:}\,GBE_e, -3/2, \#1)}\right]^{-5/3}. \qquad (21)$$

These expressions show that the large electromagnetic–gravitational hierarchy is reproduced exactly from the conformal factor ν_{cf} together with the rational powers of 3 and 2, and its associated integer algebraic combinations. In this sense, the hierarchy is encoded not by introducing new parameters, but through powers of the individual observed scalars themselves without direct knowledge of the other. The lattice encodes the perfect dimensionless hierarchy scaling information.

All admissible higher-order rational approximants for the same constant pair reproduce the identical ratio when the corresponding D_r and ν_{cf} values are used. The same construction can be applied to any pair of benchmark constants, yielding a network of exact interlocking mutual scaling relations.

Thus, within the present framework, the familiar large force hierarchy appears as a structured consequence of low-order rational scaling rather than as an isolated numerical ratio.

3.7 Explicit demonstration of the NU frequencies and lattice scalars

Tables 9–12 compare the NU frequency values of the benchmark hydrogen constants with their corresponding dimensionless lattice-scaled values in the $\mathbb{Z}^2$ representation. These two numerical scalar descriptions are not identical, but are related through the conformal factor v_{cf}, while preserving the same underlying ratios and rational exponents. One is a perfect lattice dimensionless power law, the other NU is near perfect. The NU perspective represents the physical quantities directly in Hertz, whereas the lattice perspective gives the renormalized dimensionless scalar pure mathematical values that satisfy the exact rational power-law relation on the integer grid. In this sense, the transformation by v_{cf} maps the continuous physical-frequency domain into the discrete lattice domain and vice versa.

Tables 9 and 10 are for the branches with $v_{\mathrm{cf}} < 1$, namely $(R_\infty : \mathrm{GBE}_e)$and $(R_\infty : a_0)$. Here, the lattice scalars are larger than the original NU frequencies (after normalization). In contrast, Table 11 shows the electron branch $(R_\infty : e)$, where $v_{\mathrm{cf}} > 1$, and the lattice values are smaller than the NU values. Table 12 is the proton branch $(R_\infty : p)$, where $v_{\mathrm{cf}} < 1$, so the lattice values are slightly rescaled upwards. In each case, the rescaled lattice values obey an exact rational relation, as dictated by the leading exponent: $-3/2$, $6/5$, $4/3$, and $3/2$, respectively. So, while the numerical values are different in the NU and lattice views, the hierarchy is maintained and expressed in a parsimonious exact integer-power relation. The NU domain the powers are irrational. The lattice domain powers are rational. They both define the identical physical systems from a slightly different perspective.

Table 9. Comparison of NU frequency values and corresponding $\mathbb{Z}^2$lattice scalars for the $(R_\infty : \mathrm{GBE}_e)$pair with leading exponent $-3/2$.

v_{cf} = 7.85741 10^{-1}	NU perspective	$\mathbb{Z}^2$ perspective
(R_∞: *GBEe*)	3.2898421(6.54) 10^{15} Hz	4.186931778 10^{15}
i/j = -3/2	2.90025 × 10^{-24} Hz	3.691103076 10^{-24}

Table 10. Comparison of NU frequency values and corresponding $\mathbb{Z}^2$lattice scalars for the $(R_\infty : a_0)$pair with leading exponent $6/5$.

v_{cf} = 2.172463427308 10^{-1}	NU perspective	$\mathbb{Z}^2$ perspective
(R_∞: a_0)	3.2898421(6.54) 10^{15} Hz	1.514337164 10^{16}
i/j = 6/5	5.665256408 10^{18} Hz	2.607756861 10^{19}

Table 11. Comparison of NU frequency values and corresponding $\mathbb{Z}^2$lattice scalars for the $(R_\infty : e)$pair with leading exponent $4/3$

v_{cf} = 6.209791852456 10^{1}	NU perspective	$\mathbb{Z}^2$ perspective

(R_∞: e)	3.2898421(6.54) 10^{15} Hz	5.297829916 10^{13}
i/j = 4/3	1.2355900198 10^{20} Hz	1.989744663 10^{18}

Table 12. Comparison of NU frequency values and corresponding $\mathbb{Z}^2$lattice scalars for the (R_∞: p)pair with leading exponent $3/2$.

ν_{cf} = 6.917654065768 10^{-1}	NU perspective	$\mathbb{Z}^2$ perspective
(R_∞: p)	3.2898421(6.54) ×10^{15} Hz	4.755719314 ×10^{15}
i/j = 3/2	2.268731817 10^{23} Hz	3.279626006 10^{23}

3.9 Higher-Order Isomorphic Power Laws

Beyond the first and most parsimonious rational approximation (#1), the integer search yields an infinite hierarchy of higher-order rational approximants that also satisfy the scaling constraints, Eqs. (22)–(26). Similar sequences arise for all benchmark constants; here we focus on the (R_∞, GBE_e) pair as a representative case. Each admissible fraction i/j possesses its own transformation factor ν_{cf}, while reproducing the same exact electromagnetic–gravitational hierarchy ratio and the same derived value of ν_{GBE_e}.
Representative examples are

$$\nu_{GBE_e} = \nu_{cf}\left(RH{:}\,GBE_e, -\frac{3}{2}, \#1\right)^{5/2} \nu_{RH}^{-3/2}, \qquad (22)$$

$$\nu_{GBE_e} = \nu_{cf}\left(RH{:}\,GBE_e, -\frac{23}{15}, \#2\right)^{38/15} \nu_{RH}^{-23/15}, \qquad (23)$$

$$\nu_{GBE_e} = \nu_{cf}\left(RH{:}\,GBE_e, -\frac{26}{17}, \#3\right)^{43/17} \nu_{RH}^{-26/17}, \qquad (24)$$

$$\nu_{GBE_e} = \nu_{cf}\left(RH{:}\,GBE_e, -\frac{29}{19}, \#4\right)^{48/19} \nu_{RH}^{-29/19}, \qquad (25)$$

$$\nu_{GBE_e} = \nu_{cf}\left(RH{:}\,GBE_e, -\frac{32}{21}, \#5\right)^{53/21} \nu_{RH}^{-32/21}. \qquad (26)$$

These relations are termed *isomorphic* because they represent different mathematical parameterizations of the same physical scaling relation. As the rational exponent changes, the associated value of ν_{cf} adjusts so that the observable quantity remains invariant.
As expected from Diophantine approximation theory, larger integers generally yield closer approximations to the exact irrational logarithmic slope, but with reduced parsimony. The first-order solution therefore remains the preferred representation, since it captures the same relation with the smallest integer structure.

Although the higher-order forms are mathematically valid and illustrate the infinite internal structure of the framework, they do not introduce new physical predictions beyond the leading approximation. Their primary significance is to demonstrate that the proposed hierarchy admits a consistent sequence of equivalent rational realizations. Prime-factor decompositions of these higher-order solutions are summarized in Table 13.

3.10 Evaluation of the $i, j, j-i, j+i$, and D_r values of the higher-order isomorphic power laws

Table 13 lists representative irreducible integer pairs (i, j), their associated rational exponents i/j, and the corresponding Diophantine residuals

$$D_r = \exp(R_\infty : GBE_e) - \frac{i}{j},$$

where the exact logarithmic scaling exponent is

$$\exp(R_{H\infty} : GBE_e) = -1.516871761.$$

The table also lists the integer pairs $j-i$ and $j+i$ which appear in the transformed power-law expressions, and are helpful in detecting arithmetic structure, irreducibility, and prime-factor constraints.

Table 13. Shows representative higher-order irreducible integer pairs (i, j), for the $(R_H : GBE_e)$ system, listing $j-i$, $j+i$, rational exponents i/j, and Diophantine residuals $D_r = \exp(R_H : GBE_e) - i/j$, showing convergence toward the exponent -1.51687.

i	j	$j-i$	$j+i$	i/j	$D_r = \exp(R_H : \mathrm{GBE}_e) - i/j$
−3	2	5	−1	−1.500000000	-1.68718×10^{-2}
−23	15	38	−8	−1.533333333	$+1.64616 \times 10^{-2}$
−26	17	43	−9	−1.529411765	$+1.25400 \times 10^{-2}$
−29	19	48	−10	−1.526315789	$+9.44403 \times 10^{-3}$
−32	21	53	−11	−1.523809524	$+6.93776 \times 10^{-3}$
−35	23	58	−12	−1.521739130	$+4.86737 \times 10^{-3}$
−38	25	63	−13	−1.520000000	$+3.12824 \times 10^{-3}$
−41	27	68	−14	−1.518518519	$+1.64676 \times 10^{-3}$
−44	29	73	−15	−1.517241379	$+3.69618 \times 10^{-4}$
−47	31	78	−16	−1.516129032	-7.42729×10^{-4}
−50	33	83	−17	−1.515151515	-1.72025×10^{-3}
−53	35	88	−18	−1.514285714	-2.58605×10^{-3}
−56	37	93	−19	−1.513513514	-3.35825×10^{-3}
−59	39	98	−20	−1.512820513	-4.05125×10^{-3}
−62	41	103	−21	−1.512195122	-4.67664×10^{-3}
−65	43	108	−22	−1.511627907	-5.24385×10^{-3}
−73	48	121	−25	−1.520833333	$+3.96157 \times 10^{-3}$
−79	52	131	−27	−1.519230769	$+2.35901 \times 10^{-3}$
−85	56	141	−29	−1.517857143	$+9.85381 \times 10^{-4}$
−91	60	151	−31	−1.516666667	-2.05095×10^{-4}
−97	64	161	−33	−1.515625000	-1.24676×10^{-3}

With increasing integer magnitudes, the rational exponents i/j converge towards the exact irrational exponent, and the residuals D_r become smaller in magnitude. The convergence is not monotonic, but rather oscillatory, as is typical of continued-fraction and Diophantine

approximations. Consequently, the admissible fractions oscillate about the exact value while successively reducing the residual scale.

The first entry, $-3/2$, is the most economical approximation and is the preferred solution highlighted in this paper. Successive entries such as $-23/15$, $-26/17$, and $-29/19$ offer successively better, but less parsimonious, representations of the scaling relation. An interesting aspect of the admissible sequence is its continued low-integer arithmetic. For each entry, at least one of the set of numbers $\{i, j, j-i, j+i\}$ remains a small or prime integer, maintaining some degree of simplicity in higher order. This is a consequence of the lattice solutions, rather than random rational sampling. Table 13 thus shows that the proposed hierarchy is not limited to a single fraction, but is part of an ordered infinite set of irreducible rational approximants to the same exact logarithmic exponent.

3.11 Evaluation of the i, j, D_r, v_{cf}, values of the dimensionless ref/target isomorphic power laws

Evaluation of the i/j, D_r, and v_{cf} values of the dimensionless reference/target isomorphic power laws

Table 14. A sample of higher-order isomorphic power laws for the $(R_H{:}\,\mathrm{GBE}_e)$ system, with irreducible rational exponents i/j, decimal values, Diophantine residuals D_r, conformal factors v_{cf}, and the identical hierarchy ratio $v_{RH}/v_{GBE_e} = 1.13433 \times 10^{39}$ reproduced by each solution.

i/j	Decimal i/j	$D_r = \exp(R_H{:}\,\mathrm{GBE}_e) - i/j$	$v_{cf}(R_H{:}\,\mathrm{GBE}_e, i/j)$ [Hz]	$\left[\frac{v_{ref}}{v_{cf}\left(ref{:}\,target, -\frac{i}{j}\right)}\right]^{(j-i)/j}$
−3/2	−1.5000 00000	-1.68718×10^{-2}	7.85741×10^{-1}	1.13433×10^{39}
−23/15	−1.5333 33333	$+1.64616 \times 10^{-2}$	1.26133	1.13433×10^{39}
−26/17	−1.5294 11765	$+1.25400 \times 10^{-2}$	1.19379	1.13433×10^{39}
−29/19	−1.5263 15789	$+9.44403 \times 10^{-3}$	1.14290	1.13433×10^{39}
−32/21	−1.5238 09524	$+6.93776 \times 10^{-3}$	1.10320	1.13433×10^{39}
−35/23	−1.5217 39130	$+4.86737 \times 10^{-3}$	1.07140	1.13433×10^{39}
−38/25	−1.5200 00000	$+3.12824 \times 10^{-3}$	1.04535	1.13433×10^{39}
−41/27	−1.5185 18519	$+1.64676 \times 10^{-3}$	1.02364	1.13433×10^{39}

−44/29	−1.5172 41379	+3.69618 × 10^{-4}	1.00526	1.13433 × 10^{39}
−47/31	−1.5161 29032	−7.42729 × 10^{-4}	9.89508 ×10^{-1}	1.13433 × 10^{39}
−50/33	−1.5151 51515	−1.72025 × 10^{-3}	9.75859 × 10^{-1}	1.13433 × 10^{39}
−53/35	−1.5142 85714	−2.58605 × 10^{-3}	9.63918 × 10^{-1}	1.13433 × 10^{39}
−56/37	−1.5135 13514	−3.35825 × 10^{-3}	9.53384 × 10^{-1}	1.13433 × 10^{39}
−59/39	−1.5128 20513	−4.05125 × 10^{-3}	9.44023 × 10^{-1}	1.13433 × 10^{39}
−62/41	−1.5121 95122	−4.67664 × 10^{-3}	9.35650 × 10^{-1}	1.13433 × 10^{39}
−65/43	−1.5116 27907	−5.24385 × 10^{-3}	9.28117 × 10^{-1}	1.13433 × 10^{39}
−73/48	−1.5208 33333	+3.96157 × 10^{-3}	1.05776	1.13433 × 10^{39}
−79/52	−1.5192 30769	+2.35901 × 10^{-3}	1.03402	1.13433 × 10^{39}
−85/56	−1.5178 57143	+9.85381 × 10^{-4}	1.01408	1.13433 × 10^{39}
−91/60	−1.5166 66667	−2.05095 × 10^{-4}	9.97092 × 10^{-1}	1.13433 × 10^{39}
−97/64	−1.5156 25000	−1.24676 × 10^{-3}	9.82448 × 10^{-1}	1.13433 × 10^{39}

While the rational exponents differ along the admissible sequence, each entry reproduces the same electromagnetic-gravitational hierarchy ratio,

$$\frac{\nu_{RH}}{\nu_{GBE_e}} = 1.13433 \times 10^{39},$$

showing the isomorphism of the construction. The exponent and the transformation factor are modified in such a way that the final dimensionless ratio is unchanged.

An important implication of Table 14 is that a large number of different integer power laws correspond to the same physical hierarchy. Thus, the electromagnetic-gravitational ratio is not associated with a single rational exponent, but rather with an ordered sequence of equivalent forms. In terms of economy, the first solution $-3/2$ is still the most favored form because it yields the exact ratio with the smallest integers, and hold geometric significance with the lattice. The higher-order solutions essentially display the arithmetic structure of the system.

3.12 Inverse Modulus Diophantine Spectrum of an irrational system

The Diophantine residuals do not monotonically decrease with increasing integer values. Rather, they oscillate towards zero, as is typical of rational approximations to an irrational exponent. This is shown in Figs. 9–11 for the $(R_H{:}\,\mathrm{GBE}_e)$ system. To display the local minima of the residuals, we use the inverse value $1/|\,D_r\,|$. In this case, good rational approximants are represented by high peaks, as the inverse-modulus is large for small residuals. Thus, each peak corresponds to an admissible lattice solution, a new i/j approximation and its associated v_{cf}.

Figure 9. Local view of the inverse-modulus Diophantine spectrum $1/|\,D_r\,|$ for the $(R_H{:}\,\mathrm{GBE}_e)$ system. as a function of denominator j, showing the first sequence of admissible peaks associated with rational approximants.

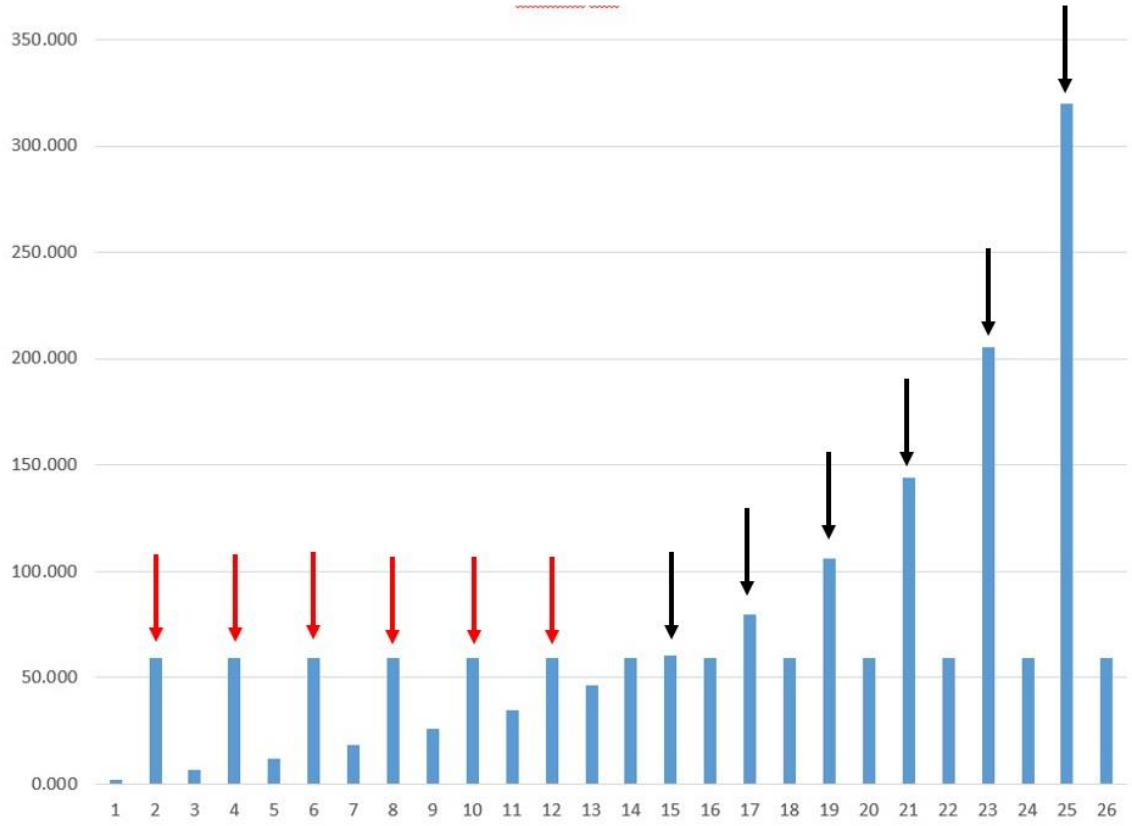

Figure 9 shows a local view of the first sequence of peaks as a function of j. The first dominant solution is the low-order fraction -3/2, followed by higher-order admissible solutions at higher denominators. Periodic repetition of degenerate solutions and new irreducible approximants occur at integer intervals, red arrows. New unique i/j values are labeled with black arrows. Each arrow is associated with a convergence point and a valid unique power law.

Figure 10. Extended inverse-modulus Diophantine spectrum $1/D_r$ for the $(R_H{:}\,\mathrm{GBE}_e)$ system over larger j range showing alternating extrema and higher-order peak structure.

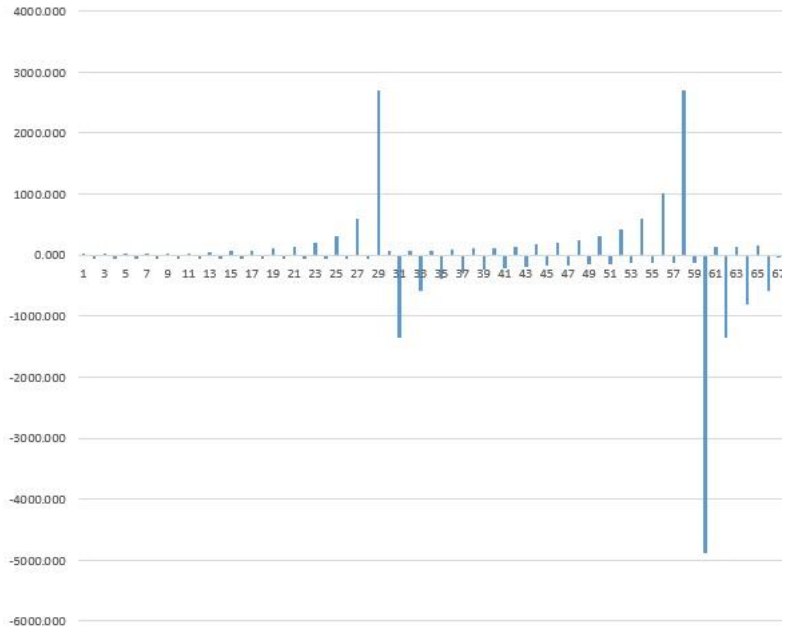

Figure 10 shows the spectrum for larger j which includes a wider range of alternating positive and negative extrema. The change in sign is due to the successive rational approximants crossing the exact irrational exponent, leading to the expected alternating convergence of continued-fraction theory.

Figure 11. Three-dimensional view of the inverse-modulus Diophantine spectrum for the $(R_H : \mathrm{GBE}_e)$ system above and below the $\mathbb{Z}^2$ lattice plane, displaying the manifold of successive rational approximants. This is a three dimensional view of Fig. (10).

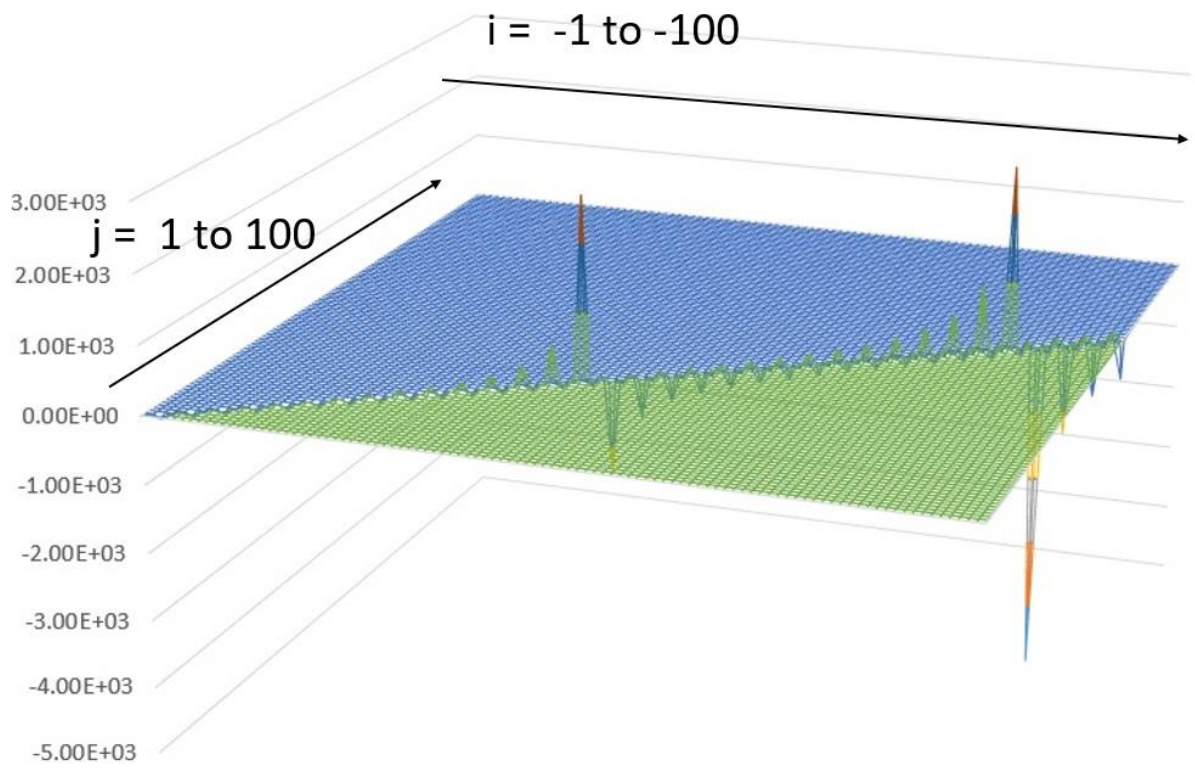

Figure 11 shows the same structure as a three-dimensional surface above and below the $\mathbb{Z}^2$ lattice plane, Fig (10). The peaks and ridges represent particularly good approximants, while the flatter areas represent less good rational fits. The resulting structure has self-similar geometric features, in accord with the recursive nature of Diophantine approximation.

These images demonstrate that the irrational exponent is not associated with random residual behavior, but with a highly structured approximation spectrum of successive integer lattice convergences.

3.13 Inverse Modulus Diophantine degenerate spectrum of a rational system

If the exact scaling exponent is rational, rather than irrational, the Diophantine residual spectrum is different. Rather than a nested sequence of successively better approximants, the residuals form an exact repeating lattice of equivalent integer multiples of the same rational fraction. This results in a degenerate spectrum with an infinite number of integer pairs that exactly obey the scaling law.

Figure 12. Three-dimensional inverse-modulus Diophantine spectrum $1/|D_r|$ for the rationalized system $(R_\infty/v_{\mathrm{cf}}: \mathrm{GBE}_e/v_{\mathrm{cf}})$. All exact convergences occur along the degenerate family $-(3n)/(2n)$, corresponding to the fundamental ratio $-3/2$, with formally divergent peaks where $D_r = 0$. n equals a consecutive integer series beginning at 1.

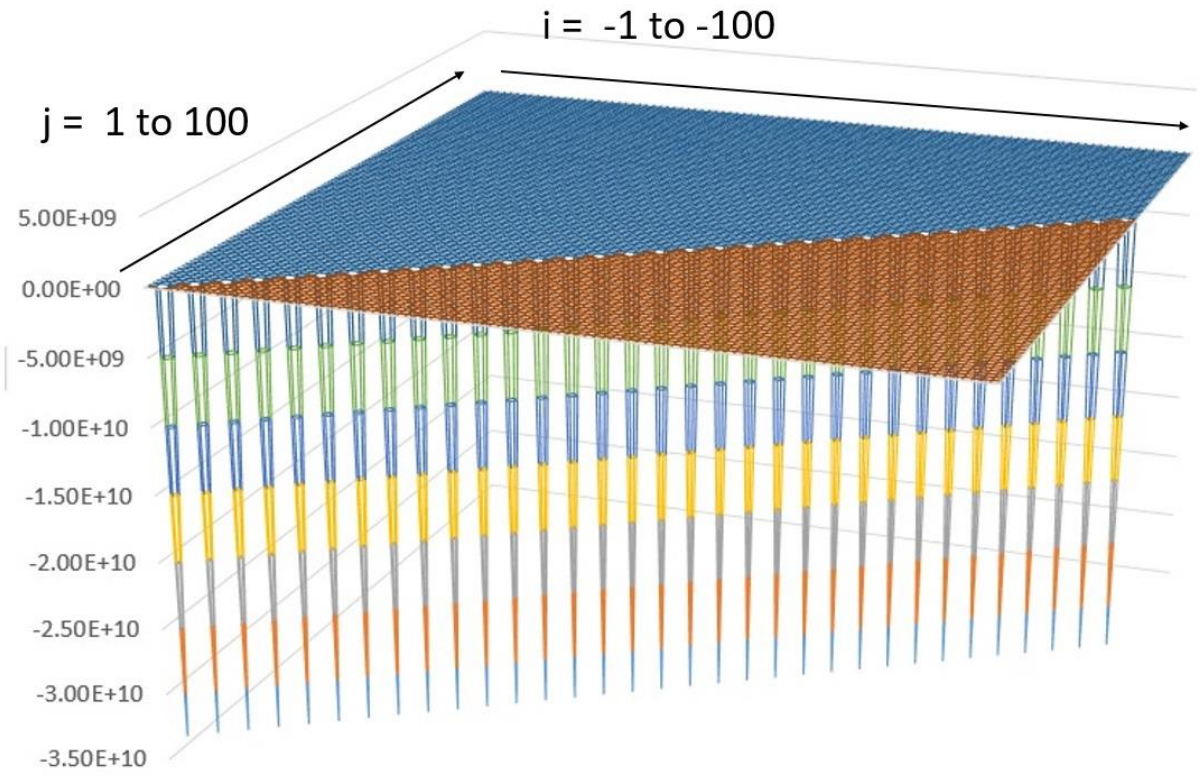

Figure 12 illustrates this behavior for the transformed system $(R_\infty/v_{\mathrm{cf}}{:}\,\mathrm{GBE}_e/v_{\mathrm{cf}})$, where the conformal scaling removes the irrational component and maps the relation onto a rational exponent. In this case, all admissible solutions lie on the family of equivalent fractions associated with the fundamental ratio $-3/2$, i.e. $-(3\cdot n)/(2\cdot n)$ for the consecutive integer series n.

These pairs satisfy the power law exactly, the residuals obey $D_r = 0$, and therefore the inverse-modulus quantity $1/|\,D_r\,|$formally is infinity. Numerically, these appear as extremely large spikes limited only by computational precision. Unlike the fractal spectrum of the irrational case (Figs. 9–11), no alternating hierarchy or irregular peak progression remains. This provides a useful contrast between irrational and rational systems. Irrational exponents generate structured, but non-degenerate approximation spectra, whereas rational exponents collapse to exact commensurate lattice families. The transformation therefore demonstrates how the original irrational hierarchy can be renormalized into a perfect rational power-law manifold. The hierarchy defining the scale of two constants is collapsed into to rational fraction.

4. Discussion

The above results reveal a hierarchy of rational scaling relations between the chosen constants of the hydrogen system in the unified frequency representation. It can be criticized that the choice of hydrogen is inappropriate, but it encompasses a range of constants that span all of the forces and particle groups. We are starting with the simplest system and intend on analyzing all of the

constants. Hydrogen is the most stable and universal element of the universe so we feel it is a valid choice. The question is whether these relations are physically meaningful or merely a mathematical artefact. In this section, we discuss the interpretive status, merits and limitations of the method, and whether the hierarchy that emerges may reflect an inherent hierarchy among the constants themselves.

4.1 Method's validity: do the emergent rational exponents and v_{cf} from the Minkowski construction reflect physical hierarchy?

This approach is novel, so it is reasonable to be suspicious of its physical significance. The pairs of integers i/j, exponents and residuals are not free parameters, but are determined solely by the numerical inputs. The question is not whether these exist, but whether they represent physical/ mathematical reality or numerical accident.

Power-law structure is ubiquitous in physics, with exponents often reflecting symmetry, hierarchy or renormalization. In this regard, the search for simple rational approximants is not unprecedented. The new idea is that a collection of fundamental constants, expressed in a common format, might display an internally coherent exponent spectrum subject to arithmetic parsimony and other limitations of Number Theory.

In the case of the hydrogen benchmark considered here, the best admissible approximants are simple fractions with low order and small integer numerators and denominators, and the transformation residuals are small. The largest and single D_r is in the range of 10^{-2}. All the others are 10^{-3} to the smallest of 10^{-5}. These are reflects as v_{cf} Hz values. These values if random should extend into the hundreds of thousands in range, but the largest encountered in these constant is 62. This is not trivial. The products of the normalized v_{cf} values of the hydrogen constants are 1.5579, 10.275; 11.501; 228.21; and 525.88. Based on the Monte Carlo results these values also can extend into many thousands for a random system. The first three a clearly not random results, particlually the 1.55 result. The two for GBE_e and p both generate the same absolute i/j values indicating structure. For constants spanning a scale of 10^{46} this is a significant finding. The fact that these same two references have maximum j values of 128 and 129 are also clearly not a typical random event. The fact that both of these findings occur with the same references is doubly non-random in character. This supports the hypothesis that the constants are an organized near perfect power law system. Simple fractions are easily found in random searches, but consistent series of the smallest prime factors, and v_{cf} values near 1 Hz are much more constrained. In the future as more constants are evaluated using the same methods if the results continue to demonstrate v_{cf} values near 1 then every added constant increasing the likelihood that the system is non-random. This is essentially guaranteed since many of the constants near the scale of the proton that will lead to large j values and v_{cf} values near 1.

The role of v_{cf} is particularly important. It is not an adjustable fitting constant, but is related to the difference between the exact logarithmic exponent and its rational approximation that simultaneously define the emergent powers. It thus connects the rational lattice to the physical scaling continuum. When $v_{cf} = 1$, the relation approaches a perfect power law, and deviations from unity measure the correction. These findings do not yet constitute a new law of physics. They

currently show that the selected constants can be represented arithmetically in a compact form with statistically unusual non-random structure under the tests applied. It remains to be seen whether this reflects fundamental physics, redundancy among the constants, or merely a representation artifact, through further tests on other systems.

All of the known constants first convergences based on the proton or GBE are within a partial harmonic power law structure based solely on their relative ratio of their log scales. This observation does have physical significance since these are the exact powers associated with a classical resonant node system. If these results are supported then the constants represent a unified resonant power system which is within the Standard Model mechanisms. The hydrogen constants e, a_0 and R_∞ can be viewed equally supported from both sides between the *GBE* and p within a mirror like hydrogen resonant cavity.

So, the current work should be regarded as a hypothesis generator: it suggests scaling regularities with structure that should be investigated, rather than a final unification of quantum and gravitational physics.

4.2 A new perspective on the mass-force hierarchy

A long-standing puzzle in physics is the hierarchy between the electromagnetic and gravitational forces. The current approach was designed to investigate whether this hierarchy can be expressed in terms of simple arithmetic scaling. In the case of hydrogen, the ratio of order 10^{39} arises from low-order power-law relations between GBE_e, e, p, and R_∞ (Eqs. 16–18). Although these quantities are not independent inputs, the SM does not offer a similarly simple internal representation of this hierarchy. This is just one example of a total of 20 different similar results. All of the ratios of one constant to any other are encoded in this integer system utilizing either constant as the base scalar.

An interesting aspect of the leading solution is that the absolute exponent of the gravitational term matches that of the proton sector under the given representation. Whether this is a physical or numerical coincidence is not clear, but it implies that the hierarchy of forces may have nontrivial symmetries when expressed in dimensionless scaling form. This is predictable since the two scalars for gravity and the proton are near exact reciprocals. This must be associated with inverse sign i/j when the references are flipped. The point is not to replace or disprove, but to supplement existing theory. The SM describes the dynamics and symmetries of interactions, but does not explain the values of particle masses or interaction hierarchies [40]. The current approach, on the other hand, seeks to determine whether the values are also organized by an additional arithmetic structure that is revealed only after rescaling on a common isomorphic basis, and evaluating them from a power law perspective. The isomorphic perspective does not change the scalars only redefines them in terms of integers.

4.3 Number theory and the mass-force architecture

The current approach postulates that some of the observed mass-force hierarchy may be due to arithmetic structure, as well as physics. There are many examples of number theory and set theory within the SM. An example is the Hofstadter butterfly which is related to a crystal lattice and the

magnetic length. This is a cornerstone in the study of fractal energy levels and the Quantum Hall Effect. This is a system interfacing rational and irrational physical systems. Although this is a novel idea, mathematics has often been the language in which physical laws are expressed. In this case, the question is whether the known constants can be organized in a meaningful and consistent way using simple integer relations across many constants. In this framework, the i/j lattice serves as an ordering space in which constants are assigned leading rational exponents with respect to a selected constant. The patterns seen in these results parallel those seen before. There are many examples of harmonic fractions based on consecutive integer series. An energy raised to a negative and a positive partial harmonic fraction power (±1/2) is seen in Density of States, just as 3/2 and -3/2 is in this work. Partial harmonic power laws of 3/2 and 4/3 have been described to be related the cosmic spin properties based on the scale of the proton, as well. Spontaneous organization of the partial harmonic frequencies of moon systems have been reported as well.

Together with the v_{cf} factors, these exponents reproduce the observed scales of the chosen constants under the chosen transformation. Thus, the lattice serves as a map of relative scales, rather than a substitute for physics. This is somewhat analogous to the periodic table: a numerical ordering first, then a microscopic theory. The analogy should not be pushed too far. The present scheme is much more limited and presently empirical, but it shows how mathematical classification schemes can come before theory. One of the advantages of the method is that the scheme can be constructed for different reference constants. In this work we have demonstrated an identical organization of all of the constants evaluated. The exponents and residuals will change, but the ratios will remain the same through infinite isomorphic transformations. This implies that the structure is related, rather than dependent on the choice of parameters. At the very least, the results suggest that the hydrogen-system constants considered here have a succinct number-theoretic representation. For example, the integers associated with the proton or the GBE as reference are associated with a consecutive integer series, {1,2/3,4/5,6/7}. This suggests an ordered system. Whether this is simply a re-representation of existing data or a deeper insight remains to be seen and will require further testing beyond the current benchmark.

4.3.1 Number theory and number sets

In the current approach, the allowable rational exponents are limited by the integer sets from which they are drawn. Since prime numbers are the fundamental building blocks of the integers, the prime factors of the leading i/j values offer a succinct description of the proposed mass–force hierarchy. In the case of the hydrogen R_∞ benchmark considered here, the leading first-order exponents are built from the small prime set $\{2, 3, 5\}$, and unity for the reference term. Some are the small prime set is {2,3,5,7}, while the *GBE* and *p* prime set is {2,3,5,7,43}. This could be coincidence, but could be of fundamental origin.

The leading solutions are interesting in that they are partial harmonic fractions (PHFs), that is, fractions of the form $1 \pm (1/j)$. These are the simplest low-order rational exponents that differ from the identity exponent 1, and they are consistent with the parsimony criterion. In this respect, their occurrence is a consequence of the arithmetic of the approximation scheme, rather than an independently postulated physical law. They are also related to resonant systems so there could be

a logical physical underpinning of the patterns identified. In the current data set, GBE_e, p, and e are linked to the low-order fractions $-3/2$, $3/2$, and $4/3$, while a_0 is linked to 6/5, which includes the complete set $\{2, 3, 5\}$. In contrast, other low-order fractions, such as 5/4, are not chosen as the best matches for the hydrogen constants in this case. The point here is not that every low-order fraction must be associated with a physical constant, but that the constants considered here occupy a sub-lattice of the low-order positions and follow the restriction of maximum parsimony.

More broadly, this suggests that prime-factor structure may offer an alternative arithmetic framework for relative scales of constants. Primes ensure that each constant is mathematically unique, and would avoid cross resonance with different constants if they were all present simultaneously within a single resonant system. Each constant could be within its own "prime set" silo. Whether this type of structure extends to other domains of fundamental physics remains to be seen, but the present benchmark demonstrates that it is at least possible in a nontrivial hydrogen system. Another finding is the almost reciprocal relation between the proton frequency and the gravitational binding-energy frequency of the electron in hydrogen. In the present representation, the leading exponents of the two branches have opposite sign, so that the gravitational branch is a sign-inverted copy of the proton branch. This is an interesting numerical aspect of the hydrogen benchmark. It remains to be seen whether this is a physical feature or an artefact of the present arithmetic representation. This near reciprocal relationship could be coincidental, but as shown with the Monte Carlo results it is highly unlikely to be a random finding.

4.3.2 Testing the Hypothesis.

A key question is whether the structures found here reflect underlying structure in fundamental constants or are a result of selective representation. In the absence of an underlying scaling regularity, the Minkowski procedure should yield exponents that are spread out across the integer lattice with some bias towards low-order rational values, large residuals, equal number of positive and negative fractions, no prime factor dominance, or recurrent organized patterns. Instead, the current hydrogen benchmarks produce a small set of parsimonious i/j values, dominated by partial harmonic fractions, consistent small consecutive prime spectrum, small D_r, and near-unity v_{cf} values when GBE_e and the proton are the references. To test the hypothesis, we need to go beyond the present benchmark to larger and independent sets of constants. There are many constants that cluster near the mass of the proton which would be associated with large j values and small v_{cf}. That alone implies that evaluating more constants with the proton as the reference will demonstrate even greater non-random properties, and would include many more constants. Each new constant would support that the system is more organized and less potentially random. If the product of all of the evaluated v_{cf} progressively diverge far below the random product of v_{cf} which continues to increase with each added constant then the hypothesis is supported. If the product of v_{cf} explodes with more constants then the hypothesis is false. The method is not reference-independent, but appears to be linked with either the proton or the *GBE*.

4.4 The "Checker Board" Mass Force Hierarchy

A useful aspect of the present construction is that the infinite set of admissible $(i/j, D_r, v_{cf})$ solutions can be mapped onto a single dominant lattice site. In the hydrogen case, the large resonance manifold (Tables 1-2) is reduced to a few dominant sites on the Minkowski grid (Table 3), each site being identified by a leading rational exponent and its residual structure. This is conceptually important. The scaling landscape is represented by a handful of integers, low-order prime factors and a single continuous correction factor v_{cf}. The resulting pattern is like a checkerboard of filled and empty lattice sites, with only certain sites corresponding to physically meaningful leading relations. Evaluation of these individual lattice sites for a group of physically related constants may demonstrate a global group theory pattern confirming the significance of the powers.

This is not intended to be a substitute for theory, but rather a shorthand hierarchy map. Just as the periodic table orders elements before detailing microscopic interactions, the current lattice orders relative scales via arithmetic position rather than interaction type. If such checkerboards exist for larger sets of constants, one could potentially build checkerboards for different physical sectors. Comparing the occupied sites, prime factors, and residual spectra might yield common principles or sector-specific features that clearly correlate with specific physical properties. For example, the weak and strong particles may be defined by "marker" prime factor sets unique to each group. At the very least, the hydrogen example demonstrates that a seemingly complex hierarchy can be encoded in a simple discrete structure. Whether this is a physical or merely a numerical compression is an important question for future research.

4.5. Cross-Domain Predictive Validity

One way to test the validity of a proposed organizing principle is to see if it is consistent across widely separated physical scales. Correlations between nearby scales can be trivial, but structures that span large scales are more constraining and thus more informative. In the current hydrogen benchmark, the same rational-scaling relations connect the electromagnetic binding scale of hydrogen to the gravitational binding scale of the electron, even though the latter is many orders of magnitude smaller than the former. They both have the same i/j pair. This is significant because any inconsistencies would tend to be magnified over such large-scale separations.

The top solutions also exhibit a symmetry between the proton and GBE_e sectors, with the leading exponents equal in magnitude and opposite in sign (in the present representation). It is not clear whether this is a significant symmetry or an artefact of the construction, but it is a real feature of the data. The v_{cf} is play a crucial role again: values close to unity mean that the cross-domain relation is close to a power law, while the deviations from unity measure the continuous correction needed to bridge the discrete lattice structure with the measured scales. The combination of the i/j and the v_{cf} is a mathematical representation of the particle-rational and wave-continuous-irrational duality.

These findings need to be taken with a grain of salt. They do not constitute a theory of quantum gravity, or replace the SM, which has a different domain. They do indicate that some constants

from different physical domains may have a common arithmetic representation in a common scaling basis [45]. If such inter-sector correspondences hold for other independent data sets, the approach would be predictive. If not, the current finding would be more likely a system-specific coincidence.

4.6 Significance of the dimensioned D_r related frequency v_{cf}

In traditional Diophantine analysis, the residual D_r is a dimensionless quantity that measures the closeness of an irrational exponent to a rational fraction. A novel aspect of the present approach is the introduction of a dimensioned manifestation of this residual structure in the form of the characteristic frequency v_{cf}, which translates the abstract residual structure into the physical scaling domain. This frequency is the link between two representations: the rational lattice of integer exponents and the frequency manifold of measured constants. So, v_{cf} is not an externally imposed fit, but a derived scale that is determined by the difference between the exact logarithmic exponent and its best rational approximant. When $v_{cf} = 1$ Hz, the relation is close to an exact power law. Deviations from unity measure the continuous correction needed to bring the measured values into agreement with the discrete lattice. So, v_{cf} serves as a measure of scaling accuracy.

Another significant implication is that the transformation converts an irrational exponent relation into an equivalent rationalized form without altering the observable ratio of constants. This enables the same physical hierarchy to be expressed either continuously in terms of direct ratios, or discretely in terms of one constant scalar, integer powers and v_{cf}. The present findings do not mean that v_{cf} is a new fundamental constant. It is a derived characteristic scale of the representation. It is significant in encoding the degree of fit of physical constants to simple arithmetic hierarchy. If such nontrivial v_{cf} structures are found to be common across larger data sets, this quantity may prove to be a valuable diagnostic of scaling order among fundamental constants.

4.7 The infinite number of power laws

A mathematical implication of the current approach is that each pair of constants is accompanied by an infinite number of acceptable rational approximants. In addition to the leading parsimonious relation, larger and larger integer pairs lead to further power-law representations that converge to the same exact logarithmic exponent. These additional relations are isomorphic in the sense that they yield the same observable ratio between constants, but differ only in the integer representation and the corresponding D_r and v_{cf} values. The physical hierarchy is thus preserved, despite the presence of multiple arithmetic representations. This is similar to the case in mathematics where a single number can be represented by an infinite number of increasingly complex rational numbers. The first solution is not unique, but minimal: it involves the smallest integers and thus is the most economical description.

For this reason, the higher-order solutions are mathematically correct, but contribute little additional physical information in the current interpretation. They primarily show the structure of the approximation manifold and the connection between simple and more complex rational representations. No claim is made here that the multiple representations correspond to different physical states. For the time being, they should be considered as alternative mathematical representations of the observed relation. The importance of the infinite hierarchy is thus methodological: it demonstrates that the observed scaling relations are not accidental, but members of a family of structured approximations whose simplest member is chosen by parsimony.

5. Conclusions

This study has explored whether a small set of hydrogen-system constants can be given a succinct arithmetic representation in a unified frequency representation and within the framework of the Minkowski approximation. In the current benchmark, the electromagnetic, inertial, geometric and gravitational scales are represented by a small number of low-order rational exponents and small emerging corrections. The findings indicate that some of the observed mass-force hierarchy may be expressible in terms of a constrained scaling structure rather than as an unconstrained set of independent random numerical constants. In this view, hierarchy is a consequence of parsimonious integer prime factor structure combined with the derived continuous correction factor v_{cf}, which connects the discrete lattice description to physical measurements.

Monte Carlo simulations suggest that the simultaneous occurrence of simple fractions, coherent ordering and near-perfect power scaling is highly unlikely under the random baselines considered here. These tests do not prove the existence of underlying structure, but encourage further exploration. The framework is not an alternative to the SM or physical theory. It provides an additional descriptive framework, emphasizing numerical organization rather than dynamics. It is therefore subject to external confirmation. The key test is simple: if the hypothesis is significant, similar low-complexity rational hierarchies and structured v_{cf} spectra should be found in larger and independent sets of constants. If not, the current hydrogen result should be dismissed as numerology.

References:

[1] M. Schlichenmaier, *An introduction to Riemann surfaces, algebraic curves and moduli spaces*. Berlin, Heidelberg: Springer Berlin Heidelberg. (1989).
[2] G.L.Naber, *The geometry of Minkowski spacetime*. Springer. (2012).
[3] S. A. Arrhenius, *Über die Dissociationswärme und den Einfluß der Temperatur auf den Dissociationsgrad der Elektrolyte* [*On the heat of dissociation and the influence of temperature on the degree of dissociation of the electrolytes*]. Z. Phys. Chem. 4: 96–116. (1889) doi:10.1515/zpch-1889-0408. S2CID 202553486.
[4] P. Zhao, W. Lichten, Z. X. Zhou, H. P. Layer, J. C. Bergquist, *Rydberg constant and fundamental atomic physics*. Physical Review A, 39(6), 2888. (1989).

[5] X. Zhang, Z. W. Raś, *Sound isolation by harmonic peak partition for music instrument recognition*. Fundamenta Informaticae, **78**(4), 613-628. (2007).
[6] N. Nettelmann, *Tesseral harmonics of Jupiter from static tidal response*. The Astrophysical Journal, **874**(2), 156. (2019).
[7] Muradian, R. *Regge law for celestial body*. Phys. Part. Nucl, (**28**), 1190. (1997).
[8] I. I. Satija, *The Hofstadter butterfly: bridging condensed matter, topology, and number theory*. Frontiers in Physics, **14**, 1667538. (2026).
[9] R. G. Forbes, *Physics of generalized Fowler-Nordheim-type equations.* Journal of Vacuum Science & Technology B: Microelectronics and Nanometer Structures Processing, Measurement, and Phenomena, **26**(2), 788-793. (2008).
[10] R. K. Nesbet, *Reference-state density functional theory*. The Journal of Physical Chemistry, **100**(15), 6104-6106. (1996).
[11] K. A. Olive, Particle Data Group, *Review of Particle Physics*, Chin. Phys. C **38**, 090001 (2014).
https://doi.org/10.1088/1674-1137/38/9/090001
[12] M. E. Peskin, *What is the hierarchy problem?*, Nucl. Phys. B **1018**, 116971 (2025). https://doi.org/10.1016/j.nuclphysb.2025.116971
[13] F. Vissani, *Do experiments suggest a hierarchy problem?*, Phys. Rev. D **57**, 7027–7030 (1998).
https://doi.org/10.1103/PhysRevD.57.7027
[14] G. F. Giudice, *Naturalness after LHC8*, PoS EPS-HEP2013, 163 (2013). https://doi.org/10.48550/arXiv.1307.7879
[15] K. G. Wilson, *The renormalization group and critical phenomena*, Rev. Mod. Phys. **55**, 583–600 (1983).
https://doi.org/10.1103/RevModPhys.55.583

[16] J.-P. Uzan, *The fundamental constants and their variation: observational and theoretical status*, Rev. Mod. Phys. **75**, 403–455 (2003).
https://doi.org/10.1103/RevModPhys.75.403
[17] J. D. Barrow, *The Constants of Nature* (Pantheon Books, New York, 2003). https://auass.net/wp-content/uploads/2021/01/The-Constants-of-Nature-.pdf
[18] D. B. Newell, ed., *The International System of Units (SI)*, NIST Special Publication 330 (National Institute of Standards and Technology, Gaithersburg, MD, 2019). https://nvlpubs.nist.gov/nistpubs/SpecialPublications/NIST.SP.330-2019.pdf
[19] E. P. Wigner, *The unreasonable effectiveness of mathematics in the natural sciences*, Commun. Pure Appl. Math. **13**, 1–14 (1960).
https://doi.org/10.1002/cpa.3160130102
[20] P. A. M. Dirac, *The cosmological constants*, Nature **139**, 323 (1937). https://doi.org/10.1038/139323a0
[21] P. A. M. Dirac, *A new basis for cosmology*, Proc. R. Soc. A **165**, 199–208 (1938). https://doi.org/10.1098/rspa.1938.0053
[22] Y. Koide, *A fermion–boson composite model of quarks and leptons*, Phys. Lett. B **34**, 201–205 (1982). https://doi.org/10.1016/0370-2693(83)90644-5
[23] Y. Koide, *Charged lepton mass formula: Development and prospects*, Int. J. Mod. Phys. E **16**, 1417–1426 (2007).
https://doi.org/10.1142/S0218301307006770

[24] Y. Sumino, *Family gauge symmetry as an origin of Koide's mass formula and charged lepton spectrum*, JHEP **05**, 075 (2009). https://doi.org/10.1088/1126-6708/2009/05/075
[25] G. 't Hooft, *Naturalness, chiral symmetry, and spontaneous symmetry breaking*, in *Recent Developments in Gauge Theories*, NATO ASI Series B **59**, 135–157 (1980). https://doi.org/10.1007/978-1-4684-7571-5_9
[26] L. Susskind, *Dynamics of spontaneous symmetry breaking in the Weinberg–Salam theory*, Phys. Rev. D **20**, 2619–2625 (1979). https://doi.org/10.1103/PhysRevD.20.2619
[27] G. I. Barenblatt, *Scaling, Self-Similarity, and Intermediate Asymptotics* (Cambridge University Press, Cambridge, 1996). https://doi.org/10.1017/CBO9781107050242
[28] J. D. Barrow, *Observational limits on the time evolution of extra spatial dimensions*, Phys. Rev. D **35**, 1805–1810 (1987). https://doi.org/10.1103/PhysRevD.35.1805
[29] H. Minkowski, *Geometrie der Zahlen* (B. G. Teubner, Leipzig, 1910). https://archive.org/details/geometriederzahl00minkrich/page/n1/mode/1up
[30] J. W. S. Cassels, *An Introduction to Diophantine Approximation* (Cambridge University Press, Cambridge, 1957). doi:10.1017/S0008439500024693
[31] A. Ya. Khinchin, *Continued Fractions* (University of Chicago Press, Chicago, 1964). https://archive.org/details/khinchin-continued-fractions/page/n1/mode/1up
[32] G. H. Hardy and E. M. Wright, *An Introduction to the Theory of Numbers*, 6th ed. (Oxford University Press, Oxford, 2008). https://blngcc.wordpress.com/wp-content/uploads/2008/11/hardy-wright-theory_of_numbers.pdf
[33] W. M. Schmidt, *Diophantine Approximation* (Springer, Berlin, 1980). https://doi.org/10.1007/BFb0098248
[34] K. Ireland and M. Rosen, *A Classical Introduction to Modern Number Theory*, 2nd ed. (Springer, New York, 1990). https://doi.org/10.1007/978-1-4757-2103-4
[35] M. V. Berry and J. P. Keating, *The Riemann zeros and eigenvalue asymptotics*, SIAM Rev. **41**, 236–266 (1999). https://doi.org/10.1137/S0036144598347497
[36] F. J. Dyson, *Statistical theory of the energy levels of complex systems*, J. Math. Phys. **3**, 140–156 (1962). https://doi.org/10.1063/1.1703773
[37] M. L. Mehta, *Random Matrices*, 3rd ed. (Elsevier, Amsterdam, 2004). https://arxiv.org/pdf/2009.05157
[38] A. Connes, *Noncommutative Geometry* (Academic Press, San Diego, 1994).
[39] E. Witten, *Reflections on the fate of spacetime*, Phys. Today **49**, 24–30 (1996). https://doi.org/10.1063/1.881493
[40] S. Weinberg, *Dreams of a Final Theory* (Pantheon Books, New York, 1992). https://alainconnes.org/wp-content/uploads/book94bigpdf.pdf
[41] J. Cardy, *Scaling and Renormalization in Statistical Physics* (Cambridge University Press, Cambridge, 1996). https://doi.org/10.1017/CBO9781316036440
[42] L. P. Kadanoff, *Scaling laws for Ising models near* T_c, Physics **2**, 263–272 (1966). https://doi.org/10.1103/PhysicsPhysiqueFizika.2.263
[43] M. Planck, *The Theory of Heat Radiation* (Dover Publications, New York, 1959). https://dn790000.ca.archive.org/0/items/theheatradiation00planrich/theheatradiation00planrich.pdf
[44] R. P. Feynman, R. B. Leighton, and M. Sands, *The Feynman Lectures on Physics*, Vol. I (Addison-Wesley, Reading, MA, 1964). https://www.feynmanlectures.caltech.edu/
[45] G. 't Hooft, *Dimensional reduction in quantum gravity*, arXiv:gr-qc/9310026

[46] D. Chakeres, *Ratio relationships between π Ratio Relationships between π, the Fine Structure Constant and the Frequency Equivalents of an Electron, the Bohr Radius, the Ionization Energy of Hydrogen, and the Classical Electron Radius*, Particle Phys. Insights **4**, 33–38 (2012). **https://doi.org/10.4137/ppi.s8269**
[47] D. W. Chakeres, *The harmonic neutron hypothesis*, Particle Phys. Insights **4**, 25–31 (2011). http://dx.doi.org/10.4137/PPI.S8241
[48] D. W. Chakeres, *Prediction and derivation of the Higgs boson from subatomic data*, J. Mod. Phys. **5**, 1670–1683 (2014). http://dx.doi.org/10.4236/jmp.2014.516167
[49] D. W. Chakeres and R. Vento, *Prediction and derivation of the Hubble constant from subatomic data*, J. Mod. Phys. **6**, 283–302 (2015). http://dx.doi.org/10.4236/jmp.2015.63033
[50] D. W. Chakeres and V. Andrianarijaona, *The Derivation of the Cosmic Microwave Background Radiation Peak Spectral Radiance, Planck Time, and the Hubble Constant from the Neutron and Hydrogen*, J. Mod. Phys. **7**, 573–586 (2016).
http://dx.doi.org/10.4236/jmp.2016.76060
[51] N. Metropolis and S. Ulam, *The Monte Carlo method*, J. Am. Stat. Assoc. **44**, 335–341 (1949). https://doi.org/10.1080/01621459.1949.10483310
[52] W. K. Hastings, *Monte Carlo sampling methods using Markov chains*, Biometrika **57**, 97–109 (1970). https://doi.org/10.1093/biomet/57.1.97
[53] M. E. J. Newman and G. T. Barkema, *Monte Carlo Methods in Statistical Physics* (Oxford University Press, Oxford, 1999). https://archive.org/details/montecarlomethod0000newm
[54] W. Feller, *An Introduction to Probability Theory and Its Applications*, Vol. 1 (Wiley, New York, 1968). https://archive.org/details/dli.ernet.5666
[55] E. T. Jaynes, *Probability Theory: The Logic of Science* (Cambridge University Press, Cambridge, 2003). https://doi.org/10.1017/CBO9780511790423
[56] N. Bohr, *On the constitution of atoms and molecules*, Philos. Mag. **26**, 1–25 (1913). https://doi.org/10.1080/14786441308634955
[57] H. A. Bethe and E. E. Salpeter, *Quantum Mechanics of One- and Two-Electron Atoms* (Springer, Berlin, 1957).
https://archive.org/details/quantummechanics0000hans/page/n2/mode/1up
[58] M. J. Duff, L. B. Okun, and G. Veneziano, *Trialogue on the number of fundamental constants*, JHEP **03**, 023 (2002).
https://doi.org/10.1088/1126-6708/2002/03/023
[59] M. Mitzenmacher, *A brief history of generative models for power law distributions*, Internet Math. **1**, 226–251 (2004).
https://doi.org/10.1080/15427951.2004.10129088
[60] A. Clauset, C. R. Shalizi, and M. E. J. Newman, *Power-law distributions in empirical data*, SIAM Rev. **51**, 661–703 (2009).
https://doi.org/10.1137/070710111